Polyamine Receptors Containing Dipyridine or Phenanthroline Units:Clues for the Design of Fluorescent Chemosensors for Metal

DOI: 10.1002/chem.200900283

Polyamine Receptors Containing Dipyridine or Phenanthroline Units: Clues for the Design of Fluorescent Chemosensors for Metal Ions

Carla Bazzicalupi, Andrea Bencini,* Silvia Biagini, Antonio Bianchi,* Enrico Faggi, Claudia Giorgi, Melania Marchetta, Federico Totti, and Barbara Valtancoli[a]

Dedicated to the Centenary of the Italian Chemical Society

Abstract: The synthesis of the macrocyclic receptor L1, which contains a tetraamine chain linking the 6,6′-positions of a 2,2′-dipyridine moiety, is reported. Its basicity properties and complexation features toward Cu^{II}, Zn^{II}, Cd^{II} and Pb^{II} have been studied in aqueous solutions by means of potentiometric, UV/Vis spectroscopy and fluorescence emission measurements and compared with those of ligand L2, in which a 1,10-phenanthroline moiety replaces the dipyridine unit of L1. In metal coordination, L1 shows a marked selectivity toward Cd^{II} over Zn^{II} and Pb^{II}. The crystal structures of its metal complexes shows that L1 possesses a preferential tetradentate binding site for metal cations, composed of the dipyridine unit and the two adjacent benzylic amine groups. This binding site has the proper dimension and conformation to selectively coordinate the Cd^{II} ion, as confirmed by DFT calculations carried out on the complexes. This coordinative zone is lost in L2. The rigidity of phenanthroline does not allow the simultaneous binding of both the benzylic amine groups to Zn^{II} and Cd^{II} and, in fact, one benzylic amine is not coordinated to these metal cations. The fluorescence emission properties of the L1 and L2 complexes are strongly pH dependent. Only the Zn^{II} and Cd^{II} complexes with L1 display fluorescence emission at neutral pH. This feature is related to the formation in solution at pH 7 of emissive protonated complexes of the type $[M(H_xL)]^{(2+x)+}$ ($x = 1$–3), in which all the nitrogen donors are involved in metal or proton binding. The emissive characteristics of these protonated complexes are confirmed by the fluorescence emission spectra collected on the $[Zn(HL1)Br][ClO_4]_2$ and $[Cd(HL1)Br][ClO_4]_2$ solid compounds dissolved in CH_3CN. Conversely, the Zn^{II} and Cd^{II} complexes with L2 are not emissive; in fact, they contain a benzylic amine group not involved in metal or proton binding that can quench the fluorescence emission of the fluorophore, thanks to a photoinduced electron-transfer process.

Keywords: chelates · fluorescence · host–guest systems · macrocycles · sensors

Introduction

There is current interest in the development of luminescent chemosensors for analytes in aqueous solution because of their potential use in medicinal or analytical chemistry.[1] In particular, metal cations are one of the most targeted substrates due to their biological and environmental relevance.[1–21] The most common approach to the realisation of synthetic chemosensors is the design of molecules consisting of a binding and a signalling unit separated by a spacer (conjugate chemosensors) and a number of chemosensors of this type for different metal ions have been recently achieved. Among possible binding units, polyamine macrocycles are undoubtedly versatile receptors for metal cations.[22–26] In fact, depending on their structural features, they can form stable metal chelates in aqueous solution and/or act as selective complexing agents for metal cations.[11,12] From this point of view, polyamines are known for their ability to form stable complexes with metal cations of environmental or toxicological relevance, such as Cd^{II} or Pb^{II}. Fi-

[a] Dr. C. Bazzicalupi, Prof. A. Bencini, Dr. S. Biagini, Prof. A. Bianchi, Dr. E. Faggi, Dr. C. Giorgi, Dr. M. Marchetta, Dr. F. Totti, Prof. B. Valtancoli
Department of Chemistry
University of Florence
Via della Lastruccia 3
50019 Sesto Fiorentino, Firenze (Italy)
Fax: (+39) 0554573364
E-mail: andrea.bencini@unifi.it
antonio.bianchi@unifi.it

Supporting information for this article is available on the WWW under http://dx.doi.org/10.1002/chem.200900283.

nally, the insertion of hydrophilic polyamine units within a structure containing a fluorogenic unit, most often a hydrophobic moiety, can ensure the resulting receptor of good solubility in aqueous media, a relevant condition for the achievement of molecular chemosensors for analytes of biological or environmental interest. Therefore, polyamines represent, in principle, optimal candidates for the synthetic assembly of chemosensors for metal cations. On the other hand, polyamines are also double-faced ligands: if they give stable complexes with many toxic metal cations, they often present scarce selectivity. For instance, polyamines generally form complexes with Zn^{II}, Cd^{II} and Pb^{II} with a similar stability in aqueous solutions.[22,23] Furthermore, the ability of a chemosensor to bind and signal a selected metal cation depends on the characteristics of the medium in which the chemosensor is used, such as temperature and pH. In particular, the sensing ability of polyamine-based receptors can be strongly pH dependent.[8–10,13,15,17] In fact, polyamines can easily protonate in aqueous solution. Protonation of polyamine groups competes with the process of metal complexation and often leads to the formation in solution of protonated metal complexes, in which acidic protons and metal cations in solution are simultaneously bound to the receptors. Even if a number of polyamine-based fluorescent chemosensors have been recently synthesised,[1] the possible formation in solution of protonated complexes and the effect of protonation on the ability of the receptors in metal sensing have been scarcely investigated.[8–10]

We have recently reported on the metal binding and sensing ability of a series of macrocyclic ligands consisting of a phenanthroline or a dipyridine unit and a polyamine chain containing amine groups separated by ethylenic chains, such as **1**–**6** in Scheme 1.[9,27] It was found that these receptors generally show scarce thermodynamic selectivity among the Zn^{II}, Cd^{II} and Pb^{II} triad. In this paper we extend this study to similar phenanthroline- or dipyridine-based polyazamacrocycles containing amine groups separated by propylenic chains (L1 and L2 in Scheme 1). At a first glance, this structural modification may appear to be of marginal relevance to determine the binding and sensing ability of the receptors. On the other hand, it is known that the replacement of ethylenic chains with propylenic ones may affect the selectivity pattern of polyamine ligands toward transition and post-transition metals, due to the higher flexibility of the ligands as well as to the larger coordination bite displayed by amine donors separated by the longer propylenic chains.[28] Conversely, amine groups linked by propylenic chains are characterised by a stronger basicity in aqueous solution with respect to amines joined by ethylenic links.[29] Finally, it is known that dipyridine and phenanthroline display a similar binding feature toward metal cations,[30] although the possible rotation of the two rings of dipyridine around the 2,2′-bond makes dipyridine slightly less rigid than phenanthroline. In principle, this latter structural feature could also influence the coordination features and emission properties of cyclic ligands containing these units, such as L1 and L2. The aim of the present paper is to demonstrate that apparently slight structural differences, such as the presence of propylenic chains instead of ethylenic ones or the replacement of a phenanthroline unit with a dipyridine moiety, can strongly influence the selectivity and sensing properties of molecular chemosensors, focusing our attention on the coordination of Zn^{II}, Cd^{II} and Pb^{II}, which often form complexes with similar stability with polyamine receptors, and of Cu^{II}, as representative examples of transition-metal cations.

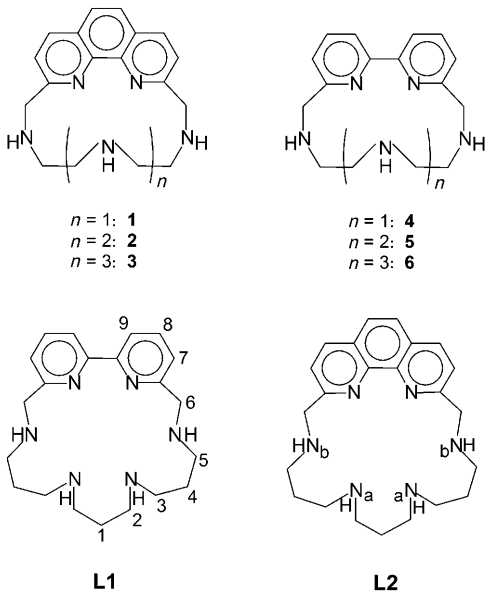

Scheme 1. Drawing of the receptors with the atom numbering used in the NMR spectroscopy experiments.

Results and Discussion

Protonation of the receptors: Since protonation of polyamine receptors is competitive with the process of metal complexation, we preliminarily carried out a study of the basicity properties of L1 and L2 by coupling potentiometric, spectrophotometric and fluorimetric measurements in aqueous solutions. The protonation constants of L2 have been previously determined in the course of a study of anion binding by L2 and its Zn^{II} complex,[31] whereas the protonation equilibria of L1 have been potentiometrically determined in this study. The basicity constants of both ligands are reported in Table 1.

Table 1. Protonation constants of L1 and L2 (298 K, 0.1 M NMe_4NO_3).

Equilibrium	Log K	
	L1	L2[a]
$L+H^+=[HL]^+$	9.94(1)[b]	10.39
$[HL]^++H^+=[H_2L]^{2+}$	8.96(2)	9.01
$[H_2L]^{2+}+H^+=[H_3L]^{3+}$	7.03(2)	7.35
$[H_3L]^{3+}+H^+=[H_4L]^{4+}$	5.95(2)	6.02

[a] From ref. [31]. [b] Values in parentheses are standard deviations on the last significant figure.

Receptors L1 and L2 display similar protonation features. As shown in Table 1, both ligands can bind up to four acidic protons in the pH range investigated (2.5–10.5) with similar protonation constants. Of note, the protonation constants are higher than those observed for the corresponding protonation equilibria in phenanthroline-containing macrocycle **2**,[27g] in which the amine groups are separated by ethylenic chains; this is in agreement with the larger $+I$ inductive effect exerted on amine groups by propylenic chains and with the higher flexibility of L1 and L2, which allow a better minimisation of the electrostatic repulsion between positive charges in the polyprotonated forms of the receptors.[29] All of the protonation constants of L1 and L2 are also higher than those reported for 2,2′-dipyridine or 1,10-phenathroline ($\log K = 4.42$ and 4.96, respectively),[30] which suggests that the heteroaromatic nitrogen atoms are not directly involved in the process of proton binding in aqueous solutions, at least in the pH range investigated. However, slow evaporation of a 0.1 M HCl aqueous solution containing $NaClO_4$ leads to crystallisation of the $[(H_{4.5}L2)(H_2O)_{0.5}Cl_{0.5}][ClO_4]_4 \cdot 2H_2O$ salt, which contains L2 in both its tetra- and pentaprotonated forms (see the Supporting Information for its crystal structure, Figure S1). This points out that the phenanthroline nitrogen atoms can be involved in proton binding at least in strongly acidic conditions.

A punctual analysis of the successive protonation steps of L1 and L2 can be carried out by recording ^{1}H NMR spectra at different pH values. The ^{1}H NMR spectrum of L1 at pH 12, in which the free amine predominates in solution, is featured by a set of nine signals, six for the aliphatic methylene protons and three for the aromatic protons; this is in keeping with a time-averaged C_{2v} symmetry, which is preserved throughout all the pH range investigated. As shown in Figure 1, formation of the mono- and diprotonated species of the ligand, $[HL1]^+$ and $[H_2L1]^{2+}$, in the pH range 11–8 is accompanied by a marked downfield shift of the signals of the methylene protons H1, H2 and H3, adjacent to N_a of the amine groups, which indicates that the first two protonation steps occur on the central nitrogen atoms of the tetraamine chain. The higher proton affinity of the N_a nitrogen atoms, in comparison with those of N_b, can be ascribed to the electron-withdrawing effect of the heteroaromatic unit on the adjacent N_b amine groups. A similar behaviour was also found for L2.[31] Therefore, both ligands feature a preferential binding zone for protons, that is, the central amine groups of the aliphatic chain, located far from the heteroaromatic units. The two successive protonation steps take place on N_b of the benzylic amine groups, as testified by the downfield shift observed for the resonances of H5 and H6 below pH 8, where the $[H_3L]^{3+}$ and $[H_4L]^{4+}$ species are formed. The resonances of the heteroaromatic protons do not show significant shifts in the pH range 12–2, indicating that protonation of dipyridine does not occur in this pH range.

This fact is confirmed by analysis of the UV spectra of L1 and L2 recorded in aqueous solutions at different pH values. In fact, their spectra are not pH dependent and are almost

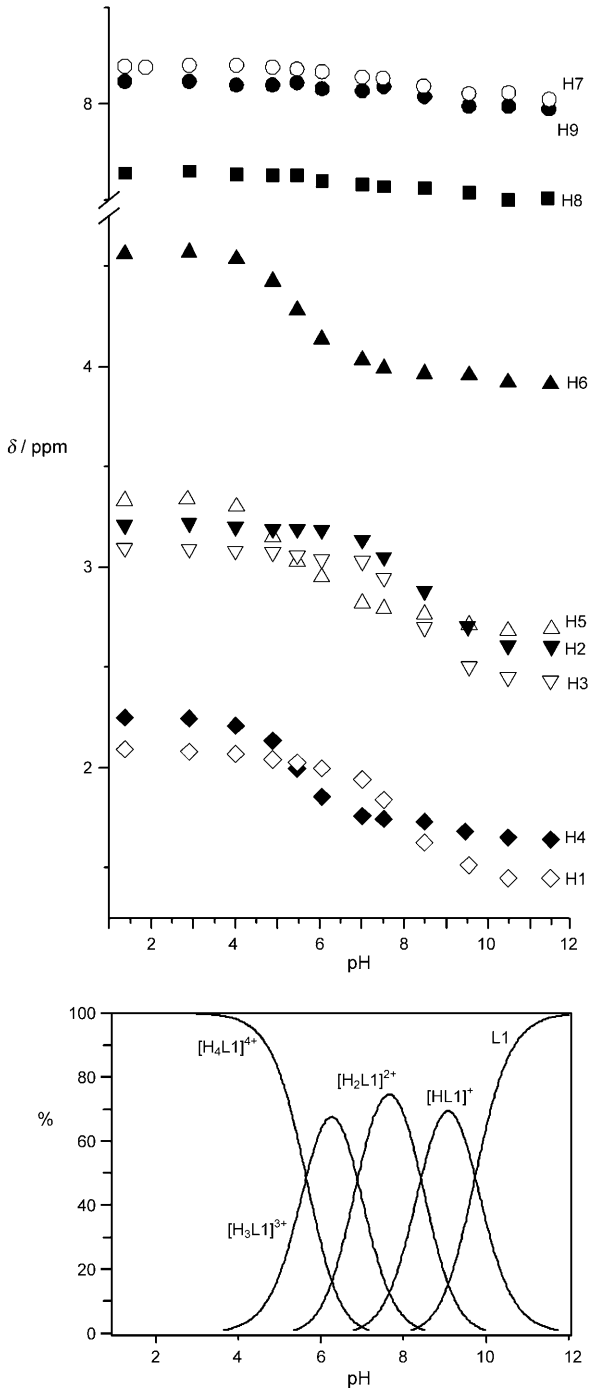

Figure 1. Top: pH dependence of the ^{1}H NMR spectroscopic signals of L1. Bottom: A distribution diagram of its protonated species (298 K, 0.1 M NMe_4NO_3).

equal to those of unprotonated 2,2′-dipyridine and 1,10-phenanthroline even at strongly acidic pH values (pH 2), whereas it is known that protonation of 2,2′-dipyridine[9d,27a,d] and 1,10-phenanthroline[32] is accompanied by remarkable red-shifts of their absorption bands at 290 and 270 nm, respectively. Conversely, the emission spectra of L2 are strongly pH dependent. As shown in Figure 2, the receptor is not emissive in alkaline aqueous solutions and shows the typical

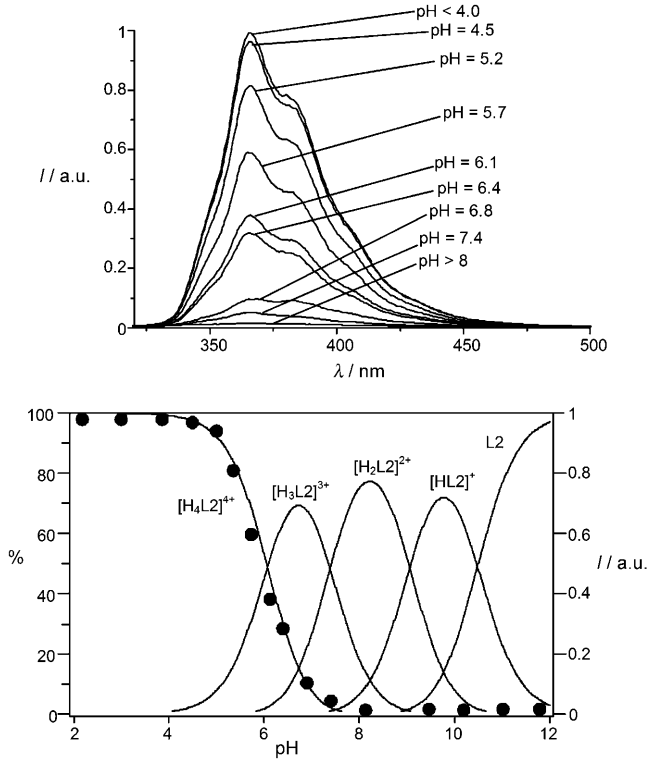

Figure 2. Top: Emission spectra of L2 at selected pH values. Bottom: pH dependence of its emission intensity at 366 nm (298 K, $\lambda_{exc}=280$ nm, 0.1 M NMe_4NO_3).

emission of phenanthroline only at acidic pH values, that is, upon protonation of the $[H_3L2]^{3+}$ species to give the $[H_4L2]^{4+}$ one. This effect can be attributed to the presence, in $[H_3L2]^{3+}$, of an unprotonated benzylic amine group (N_b in Scheme 1). In fact, as already observed in other phenanthroline-containing polyamine ligands,[9e,f] the lone pair of the benzylic nitrogen atoms, located close to phenanthroline, can efficiently quench the fluorescence emission of the fluorophore through an electron-transfer process. Finally, protonation of all amine groups of the aliphatic chain below pH 7 makes the lone pairs no longer available for the photoinduced eletctron-transfer (PET) process and gives rise to a consequent renewal of the fluorescence emission of phenanthroline.

Differently from L2, L1 displays a weak fluorescent emission even at acidic pH values, in keeping with the scarcely emissive nature of unprotonated 2,2′-dipyridine.[27a,d]

Metal complexation—structural characteristics of the complexes in the solid state: Crystals suitable for X-ray analysis of the protonated complexes $[Cu(HL1)(ClO_4)][ClO_4]_2{\cdot}H_2O$ (**a**), $[Zn(HL1)Br][ClO_4]_2$ (**b**), $[Cd(HL1)Br][ClO_4]_2$ (**c**) and $[Pb(H_2L1)Br][ClO_4]_3{\cdot}H_2O$ (**d**) were obtained by slow evaporation of slightly acidic aqueous solutions containing L1 and the appropriate metal salt in the presence of an excess of $NaClO_4$. Selected distances and angles for the metal coordination environments are listed in Table 2.

Table 2. Bond lengths [Å] and angles [°] for the metal coordination environments in $[Cu(HL1)(ClO_4)][ClO_4]_2{\cdot}H_2O$ (**a**), $[Zn(HL1)Br][ClO_4]_2$ (**b**), $[Cd(HL1)Br][ClO_4]_2$ (**c**) and $[Pb(H_2L1)Br][ClO_4]_3{\cdot}H_2O$ (**d**).

	a Cu1 (X = O5)	**b** Zn1 (X = Br2)	**c** Cd1 (X = Br1)	**d** Pb1 (X = Br1)
M–X	2.414(6)	2.366(2)	2.577(1)	2.841(1)
M–N1	1.925(4)	2.11(1)	2.341(6)	2.509(8)
M–N2	1.955(6)	2.140(9)	2.349(5)	2.518(8)
M–N3	2.037(4)	2.145(9)	2.354(5)	2.760(8)
M–N6	2.041(5)	2.148(9)	2.350(6)	2.722(7)
X-M-N6	89.8(2)	107.6(2)	103.3(1)	77.1(2)
X-M-N2	100.0(2)	112.3(2)	114.0(1)	85.9(2)
X-M-N3	91.1(2)	103.2(3)	99.6(1)	87.8(2)
X-M-N1	103.3(2)	113.0(3)	114.8(1)	82.4(2)
N6-M-N2	162.3(2)	136.3(3)	132.6(2)	128.9(2)
N6-M-N3	113.5(2)	111.4(3)	131.2(2)	157.4(2)
N6-M-N1	83.1(2)	75.7(3)	70.5(2)	64.8(2)
N2-M-N3	81.3(2)	76.4(3)	71.1(2)	65.5(2)
N2-M-N1	80.3(2)	72.8(4)	67.7(2)	65.4(2)
N3-M-N1	158.3(2)	139.1(3)	134.3(2)	130.5(2)

The crystal structures of **a**, **b**, **c**, and **d** are composed of $[Cu(HL1)(ClO_4)]^{2+}$, $[Zn(HL1)Br]^{2+}$, $[Cd(HL1)Br]^{2+}$ and $[Pb(H_2L1)Br]^{3+}$ complexed cations, perchlorate anions and, in the cases of **a** and **d**, water molecules. The **a**, **b** and **c** complexes feature similar metal coordination environments and overall ligand conformations (Figure 3a, b and c). In all these cases, the metal is coordinated by the two nitrogen atoms of dipyridine, N1 and N2, and by the amine donors N3 and N6, adjacent to the heteroaromatic unit. The remaining two amine groups (N4 and N5) are not coordinated, one of them being protonated. A perchlorate oxygen atom (O5 in **a**) or a bromide anion (Br2 in **b**, Br1 in **c**) complete the coordination sphere of the metal cations. The resulting coordination geometry can be best described as a distorted square pyramid, in which the four nitrogen atoms define the basal plane (maximum deviation from the mean plane 0.184(5) Å for N2 in **a**, 0.034(9) Å for N1 and N2 in **b** and 0.024(5) for N1 in **c**) and an exogenous oxygen atom or bromide anions occupy the apical position. The metal ions lie above the basal plane (0.3817(7) Å in **a**, 0.670(1) Å in **b** and 0.6227(7) in **c**), shifted towards the apical position, whereas the Cu1–O5, Zn1–Br2 and Cd1–Br1 axes form angles of 7.92(2)°, 5.9(2)° and 11.4(1)° with the basal plane. In the case of the **a** and **c** complexes, the Cu–N and Cd–N distances, ranging respectively from 1.925(4) to 2.041(5) Å and from 2.341(6) to 2.354(5) Å, compare well with the mean values obtained from a search on the Cambridge Structural Database (CSD)[33] for the Cu–N (2.029(1) Å) and Cd–N (2.349(1) Å) bond lengths. Conversely, three of four Zn–N bond lengths in **b** are longer than that generally observed in Zn^{II} complexes with polyaza ligands (mean value of 2.087(1) Å found by a CSD search).[33]

As far as the ligand conformation is concerned, in all three complexes the two pyridine units are not coplanar, with dihedral angles of 5.8(3)° in **a**, 12.7(5)° in **b** and 7.3(3)° in **c**. The ligand assumes a bent conformation along the N3–

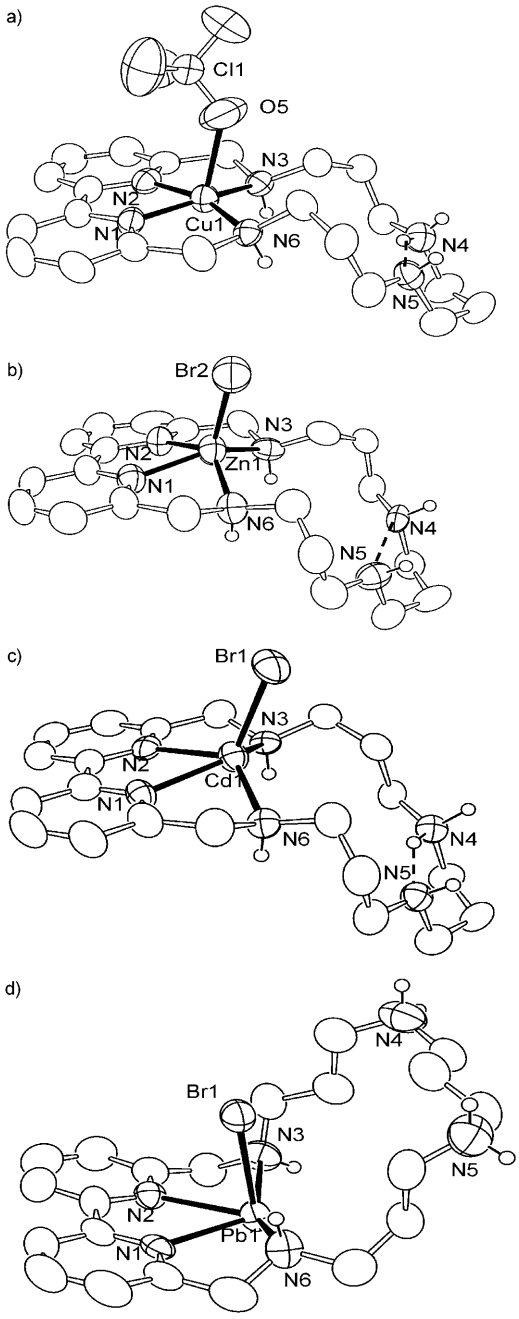

Figure 3. ORTEP drawings of the a) $[Cu(HL1)(ClO_4)]^{2+}$, b) $[Zn(HL1)Br]^{2+}$, c) $[Cd(HL1)Br]^{2+}$ and d) $[Pb(H_2L1)Br]^{3+}$ cations.

N6 axis with dihedral angles between the mean planes defined, respectively, by the four aliphatic nitrogen atoms and by the dipyridine units of 157.8(1)° in **a**, 141.8(3)° in **b** and 145.3(1)° in **c**. In the **a** and **c** complexes, the analysis of the Fourier difference maps allowed us to individuate the acidic proton, which results in being localised on the N4 amine groups. In both complexes, N4 is involved in a hydrogen bond with the adjacent N5 nitrogen atom (N4···N5 2.935(8) Å, H4···N5 2.14(5) Å, N4-H4-N5 146(5)° in **a**; N4···N5 2.818(8) Å, H2···N5 1.98(8) Å, N4-H2-N5 148(7)° in **c**). In the Zn^{II} complex **b**, the acidic proton was not localised; however, the N4 and N5 nitrogen atoms are still hydrogen bonded, as testified by the short interatomic distance (2.92(1) Å).

In the $[Pb(H_2L1)Br]^{3+}$ complex, the metal ion is, once again, pentacoordinated by the heteroaromatic and benzylic nitrogen atoms and by a bromide anion. Although the arrangement of the donor atoms around the metal can be assimilated to a square pyramid, with the nitrogen donors defining the basal plane, in this case the coordination geometry presents strong distortions from the theoretical polyhedron. For instance, the N3-Pb1-N6 angle is 157.4(2)° instead of the expected value of 90°. The Pb^{II} ion lies 0.3436(4) Å outside the basal plane; however, differently from the other L1 complexes, the metal is shifted in the opposite direction with respect to the apical position occupied by the bromide anion. The arrangement of the five donors around the metal leaves a large zone free from coordinated atoms, which is likely to be occupied by the lone pair of Pb^{2+}. Such a "gap" in the coordination geometry of Pb^{II} has been ascribed by several authors to the presence of a stereochemically active lone pair and has been found in other complexes with polyazamacrocycles containing heteroaromatic moieties.[27g,34] The Pb^{II}–N distances span from 2.509(8) to 2.760(8) Å. Two of them are around 0.2 Å longer than those generally observed in polyamine complexes with Pb^{II} (mean value of 2.577(6) Å found by a CSD search).

In the case of L2, crystals suitable for X-ray analysis were obtained only in the case of the Zn^{II} and Pb^{II} complexes. The crystal structure of the $[Zn(HL2)Br][Br][ClO_4]$ complex has been previously described.[31] The $[Zn(HL2)Br]^{2+}$ cation (Figure 4a and Table 3) presents significant differences from the corresponding L1 complex **b**. Although in $[Zn(HL2)Br]^{2+}$ the Zn^{II} ion is once again pentacoordinated by

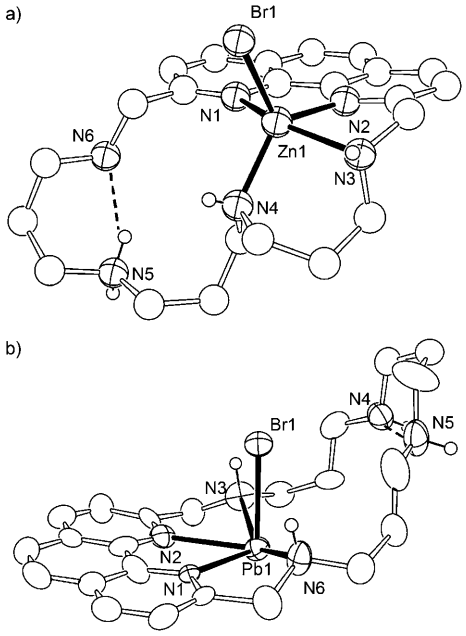

Figure 4. ORTEP drawings of the a) $[Zn(HL2)Br]^{2+}$ and b) $[Pb(HL2)Br]^{2+}$ cations.

Table 3. Bond lengths [Å] and angles [°] for the metal coordination environments in $[Zn(HL2)Br][Br][ClO_4]$ and $[Pb(HL2)Br][PF_6]_{1.5}[NO_3]_{0.5}\cdot H_2O$.

$[Zn(HL2)Br][Br][ClO_4]$[a]		$[Pb(HL2)Br][PF_6]_{1.5}[NO_3]_{0.5}\cdot H_2O$	
Zn1–Br1	2.354	Pb1–Br1	2.735(1)
Zn1–N1	2.370	Pb1–N1	2.540(9)
Zn1–N2	2.047	Pb1–N2	2.51(1)
Zn1–N3	2.276	Pb1–N3	2.69(1)
Zn1–N4	2.072	Pb1–N6	2.77(1)
Br1-Zn1-N1	99.2	Br1-Pb1-N1	90.6(2)
Br1-Zn1-N3	102.5	Br1-Pb1-N3	76.8(2)
Br1-Zn1-N2	115.2	Br1-Pb1-N2	88.4(2)
Br1-Zn1-N4	118.2	Br1-Pb1-N6	77.3(2)
N1-Zn1-N3	149.4	N1-Pb1-N3	128.8(3)
N1-Zn1-N2	75.0	N1-Pb1-N2	65.5(3)
N1-Zn1-N4	98.0	N1-Pb1-N6	62.7(3)
N3-Zn1-N2	76.4	N3-Pb1-N2	64.7(3)
N3-Zn1-N4	90.5	N3-Pb1-N6	151.7(3)
N2-Zn1-N4	126.6	N2-Pb1-N6	125.8(3)

[a] From ref. [31].

the two heteroaromatic nitrogen atoms, two amine groups (N3 and N4) and a bromide anion, one of the benzylic nitrogen atoms (N6) is not involved in metal binding. Such a difference from the **b** complex with L1 may reside in the higher rigidity of phenanthroline with respect to dipyridine. Whereas in $[Zn(HL2)Br]^{2+}$ the rigidity of the phenanthroline moiety does not allow the simultaneous coordination of both benzylic amine groups to this metal, in $[Zn(HL1)Br]^{2+}$ the loss of coplanarity between the two pyridine rings enables the ligand to assume an appropriate conformation for the simultaneous binding of both benzylic amine groups to the metal.

The crystal structure of $[Pb(HL2)Br][PF_6]_{1.5}[NO_3]_{0.5}\cdot H_2O$ (**e**) (see Figure 4b and Table 3) consists of $[Pb(HL2)Br]^{2+}$ cations, PF_6^- and NO_3^- anions and water solvent molecules. One PF_6^- and the nitrate anions lie on crystallographic C_2 axes and are in consequence only partially contained in the asymmetric unit. Both the coordination geometry and ligand conformation are very similar to those found for the Pb^{II} complex with L1, **d** (Figure 3d). In fact, the coordination environment is best described as a strongly distorted square pyramid, in which the basal plane is defined by the four nitrogen atoms (N1, N2, N3 and N6) and the apical position is occupied by the bromide anion. Once again, a zone "free" from coordinated donor atoms is clearly observable in the metal coordination environment, due to the presence of the stereochemically active lone pair of Pb^{II}.[27g,34] The ligand displays a conformation folded along the N3–N6 axis, with a dihedral angle of 143.0(2)° between the plane of phenanthroline and the plane defined by the secondary nitrogen atoms. A strong intramolecular hydrogen bond (N4···N5 2.77(2) Å) is observed between the two unbound amine donors, one of them being protonated. In this case, however, the acidic proton was not localised in the ΔF map.

Metal complexation in aqueous solutions—general features and selectivity patterns: The binding ability of the two ligands toward Cu^{II}, Zn^{II}, Cd^{II} and Pb^{II} was first analysed by means of potentiometric titrations in aqueous solutions. This was to determine the species present in solution and their formation constants (Table 4) and to establish the possible presence of a selectivity pattern among the different metal cations. Both ligands form rather stable 1:1 complexes with the metals under investigation. However, the stability constants of the $[ML1]^{2+}$ and $[ML2]^{2+}$ ($M = Cu^{II}$, Zn^{II}, Cd^{II} or Pb^{II}) complexes are 3–4 logarithmic units lower than the corresponding complexes with the hexadentate ligand **2** (see Scheme 1),[9e,27e,g] which contains a triethylentetraamine chain linking the 2,9-position of 1,10-phenanthroline. This effect can be attributed to the replacement of the ethylenic chains that link the amine groups in **2** by propylenic ones. In fact, the increased N-M-N bond angle, as a result of the larger bite of propylenic chains, may reduce the stability of the complexes.[28] As a consequence of the reduced binding ability of amine groups joined by propylenic bridges, some amine groups are probably weakly bound or not bound to the metal cations. This structural hypothesis is supported by the marked tendency of the $[ML1]^{2+}$ and $[ML2]^{2+}$ complexes to bind acidic protons in aqueous solutions, affording mono-, di- and, in some cases, even triprotonated species. In particular, the constants for the addition of the first two protons to the $[ML]^{2+}$ complexes are remarkably high, in most cases greater than 6 logarithmic units. These protonated species are of particular relevance in the solution chemistry of the present complexes because of their presence in a wide pH range, including the neutral pH region, as shown in Figure 5 for the Cu^{II} and Zn^{II} complexes with L1.

Table 4. Stability constants of the Cu^{II}, Zn^{II}, Cd^{II}, and Pb^{II} complexes with L1 and L2 in aqueous solution (0.1 M NMe_4NO_3, 298 K).

Reaction	Log K[a]			
	Cu^{II}	Zn^{II}	Cd^{II}	Pb^{II}
$M^{2+} + L1 = [ML1]^{2+}$	15.2(1)	10.85(1)	13.9(1)	8.7(1)
$[ML1]^{2+} + H^+ = [M(HL1)]^{3+}$	9.5(1)	8.01(1)	7.04(8)	8.7(1)
$[M(HL1)]^{3+} + H^+ = [M(H_2L1)]^{4+}$	5.9(1)	6.10(1)	6.05(7)	7.5(1)
$[M(H_2L1)]^{4+} + H^+ = [M(H_3L1)]^{5+}$	3.9(1)	4.5(1)	3.93(5)	–
$[ML1]^{2+} + OH^- = [M\{(OH)L1\}]^+$	2.7(1)	4.5(1)	4.01(1)	–
$[M\{(OH)L1\}]^+ + OH^- = [M\{(OH)_2L1\}]$	–	3.5(1)	–	7.4(1)
$M^{2+} + L2 = [ML2]^{2+}$	13.90(3)	9.83[b]	10.21(1)	8.6(3)
$[ML2]^{2+} + H^+ = [M(HL2)]^{3+}$	9.04(2)	8.41	8.66(1)	9.26(2)
$[M(HL2)]^{3+} + H^+ = [M(H_2L2)]^{4+}$	5.97(3)	7.15	7.20(1)	7.65(1)
$[M(H_2L2)]^{4+} + H^+ = [M(H_3L2)]^{5+}$	5.46(2)	5.30	–	–
$[ML2]^{2+} + OH^- = [M\{(OH)L2\}]^+$	–	3.90	–	3.77(3)
$[M\{(OH)L2\}]^+ + OH^- = [M\{(OH)_2L2\}]$	–	2.47	–	–

[a] Values in parentheses are standard deviations on the last significant figure. [b] From ref. [31].

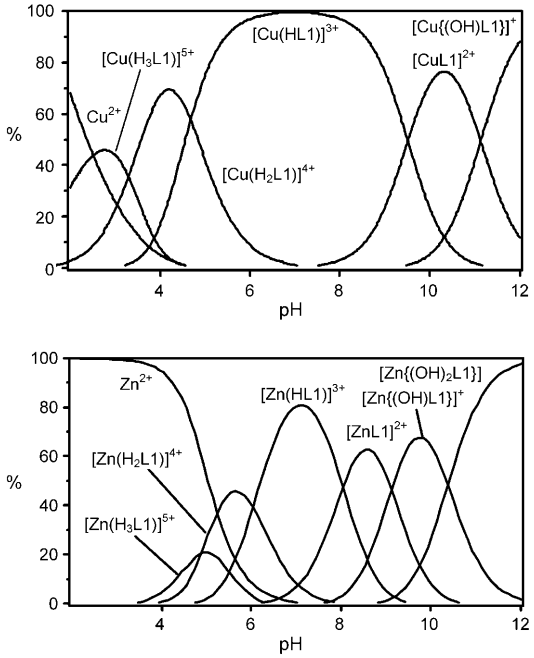

Figure 5. Distribution of the complexed species of L1 in the presence of 1 equiv of Cu^{II} (top) and Zn^{II} (bottom) ($[L]=[Cu^{II}]=[Zn^{II}]=1\times10^{-3}$ M, 298 K, 0.1 M NMe_4NO_3).

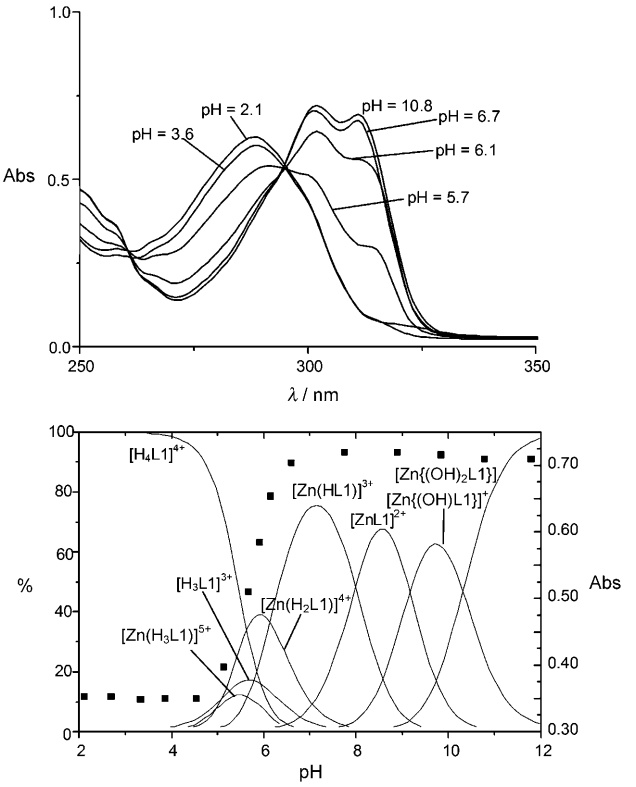

Figure 6. Top: Selected absorption spectra of L1 in the presence of 1 equiv of Zn^{II}. Bottom: Absorbance at 305 nm (■, right *y* axis) as a function of pH compared to the distribution curves of the complexes (——, left *y* axis) for a system containing L1 and Zn^{II} in 1:1 molar ratio ($[L1]=5\times10^{-5}$ M, 298 K, 0.1 M NMe_4NO_3).

To corroborate the potentiometric study, metal complexation was also followed by recording UV spectra at different pH values. In fact, the UV absorption band of 2,2′-dipyridine and 1,10-phenanthroline is markedly affected by metal coordination. In particular, metal binding to dipyridine is accompanied by the disappearance of its original band at 293 nm and the simultaneous formation of a new structured band at approximately 305 nm, whereas metal coordination by 1,10-phenanthroline may result in either a decrease (in the case of Zn^{II}, Cd^{II} and Pb^{II} complexation) or an increase (in the case of Cu^{II}) of the absorbance of its UV band at 270 nm.[9,27] These spectral changes can be used as a diagnostic tool to assess the involvement of the heteroaromatic nitrogen atoms in metal binding. As shown in Figure 6 for the Zn^{II} complexes with L1, the appearance of a new band with a maximum at 305 nm is observed above pH 4. In consequence, the absorbance monitored at 305 nm increases from pH 4 to pH 7, where the process of metal complexation occurs to form the $[Zn(H_xL1)]^{(2+x)+}$ ($x=1$–2) complexes. Finally, the band does not show significant changes in the alkaline pH region, that is, with the formation of the $[ZnL1]^{2+}$, $[Zn\{(OH)L1\}]^{+}$ and $[Zn\{(OH)_2L1\}]$ complexes. Complexation of Zn^{II} by L2 to give the protonated complexes $[Zn(H_3L2)]^{5+}$, $[Zn(H_2L2)]^{4+}$ and $[Zn(HL2)]^{3+}$ in the pH range 4–7 is accompanied by a decrease of the absorbance and by a slight redshift (around 6 nm) of the phenanthroline band at 270 nm (Figure 7). No further changes are then observed in the alkaline pH region. Similar results are also obtained with the other metal ions (see the Supporting Information, Figures S2 and S3). These data account for the involvement of the heteroaromatic nitrogen atoms in all of the different complexed species formed by L1 or L2, as is displayed by all of the crystal structures obtained for their metal complexes (see above).

The crystal structures of the complexes also show that the metal cations are coordinated by a single (in $[Zn(HL2)]^{3+}$) or both benzylic nitrogen atoms (in $[Cu(HL1)(ClO_4)]^{2+}$, $[Zn(HL1)Br]^{2+}$, $[Cd(HL1)Br]^{2+}$, $[Pb(H_2L1)Br]^{3+}$ and $[Pb(HL2)Br]^{2+}$). The remaining couple of amine donors, L1 and L2, far from the heteroaromatic moieties and characterised by a higher basicity, are probably not involved or weakly involved in metal binding in aqueous solution; they can therefore act as binding sites for the acidic protons in the protonated forms of the complexes.

If we compare the binding ability of the two ligands, Table 4 shows that the $[ML1]^{2+}$ complexes are generally more stable than the corresponding $[ML2]^{2+}$ ones, with the only exception being the Pb^{II} complexes, which display stability constants equal to those within the experimental error. The higher stability of the complexes with L1 cannot be attributed to the different binding ability of the dipyridine nitrogen atoms with respect to the phenanthroline ones, since 2,2′-dipyridine and 1,10-phenanthroline give metal chelates with almost equal stability (for instance, $\log K=9.00$ and 9.25 for the equilibrium $Cu^{2+}+L=[CuL]^{2+}$ with L = 2,2′-dipyridine and 1,10-phenanthroline, respectively).[30] On the

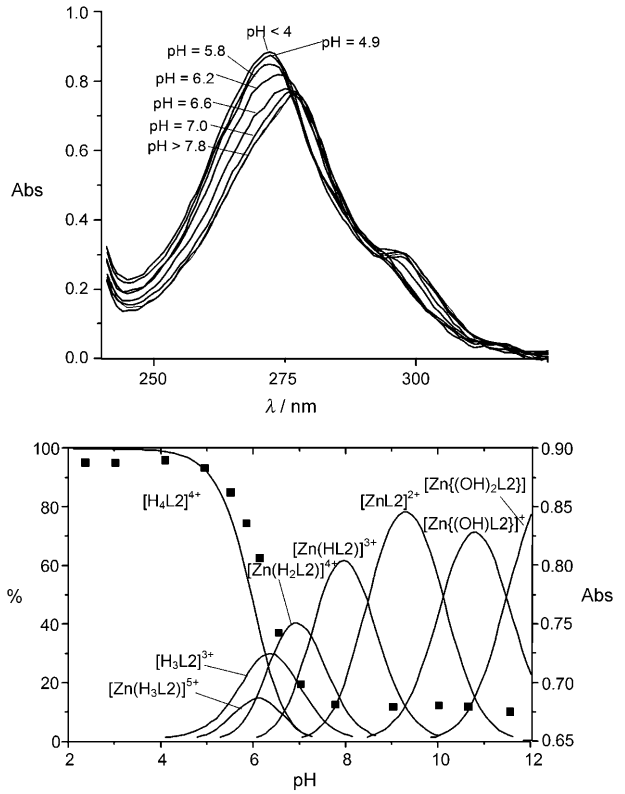

Figure 7. Top: Selected absorption spectra of L2 in the presence of 1 equiv of Zn^{II}. Bottom: Absorbance at 270 nm (■, right *y* axis) as a function of pH compared to the distribution curves of the complexes (——, left *y* axis) for a system containing L2 and Zn^{II} in 1:1 molar ratio ([L2] = 3×10^{-5} M, 298 K, 0.1 M NMe_4NO_3).

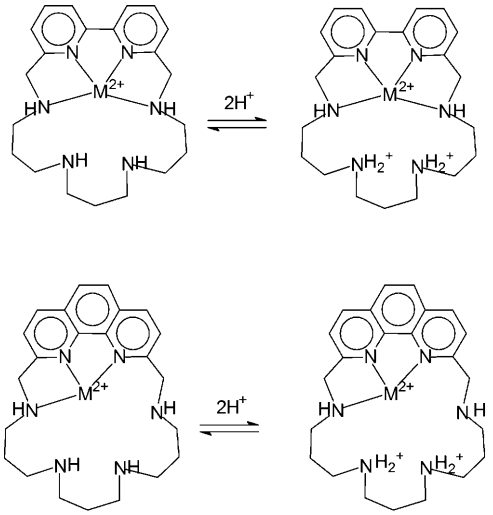

Scheme 2. Proposed binding mode of L1 in the $[ML1]^{2+}$ and $[M(H_2L1)]^{4+}$ complexes (M = Cu^{II}, Zn^{II}, Cd^{II}).

other hand, previous work on phenanthroline-containing macrocycles, such as **1**–**3**, has shown that the rigidity of the heteroaromatic unit does not allow the simultaneous coordination of the phenanthroline donors and of both the adjacent benzylic amine groups to relatively small metal cations such as Cu^{II} or Zn^{II}.[1p,9e,f,27e] This seems to be the case of L2 also. In fact, the crystal structure of the $[Zn(HL2)]^{3+}$ complex shows that only one benzylic group is bound to the metal ion. Conversely, in the complexes with L1 the possible rotation of the two pyridine rings along the 2,2′-axis of dipyridine may confer to the macrocyclic framework a somewhat higher flexibility, which allows both the benzylic amine groups to bind to the metal cations, as is shown by the crystal structures of the Cu^{II}, Zn^{II} and Cd^{II} complexes with L1. It seems likely that L1 contains a preferred binding site for metals, consisting of the dipyridine nitrogen atoms and the two adjacent benzylic amine groups (Scheme 2). This tetradentate site is lost in L2, in which one benzylic nitrogen atom is not coordinated, due to the rigidity of phenanthroline. This structural difference may lead to the higher stability observed for the L1 complexes with Cu^{II}, Zn^{II} and Cd^{II} with respect to the corresponding complexes with L2. Of note, the larger Pb^{II} cation, which appears to be coordinated in a similar tetradendate mode by both L1 and L2 (Figure 3d and Figure 4b), gives complexes of equal stability with both ligands.

Among the investigated metal ions, Cu^{II} forms the most stable complex (Table 4), as expected considering the effect of the crystal-field stabilisation energy (CFSE) in Cu^{II} coordination. The most interesting feature in Table 4, however, is the higher stability of the $[CdL]^{2+}$ complex with respect to the $[ZnL]^{2+}$ and $[PbL]^{2+}$ ones (L = L1 or L2). This effect is of particular relevance in the case of L1, in which the $[CdL1]^{2+}$ complex is more than 3 logarithmic units more stable than the corresponding Zn^{II} and Pb^{II} complexes, a rather uncommon feature with polyamine ligands, including phenanthroline or dipyridine-containing polyamine macrocycles.[9,27] However, the comparison between the binding ability of L1 or L2 toward different metal cations is complicated by the presence of overlapping protonation and deprotonation equilibria involving the $[ML]^{2+}$ complexes (Table 4). This problem can be conveniently overcome by considering a competitive system containing ligand and metal cations in equimolecular concentrations and calculating the overall percentages of the different complexed cations over a wide pH range. Plots of the percentages versus pH produces species distribution diagrams from which the binding ability of a ligand can be interpreted in terms of selectivity.[35] Figure 8 displays similar plots obtained for competitive systems containing L1 or L2 and Zn^{II}, Cd^{II} and Pb^{II}. Whereas L2 shows a poor ability to recognise a single metal cation, L1 is characterised by a marked selectivity for Cd^{II} over Pb^{II} and Zn^{II}. For instance, at pH 7 more than 95% of Cd^{II} is complexed by L1, whereas Zn^{II} is complexed at less than 5%. Pb^{II} is complexed in percentages lower than 1% all over the pH range investigated. As discussed above, in L1 the metal cations are preferentially bound by the coordination site defined by the dipyridine nitrogen atoms and the two adjacent benzylic amine groups. Most likely, selective coordination of Cd^{II} over Zn^{II} and Pb^{II} is due to a better di-

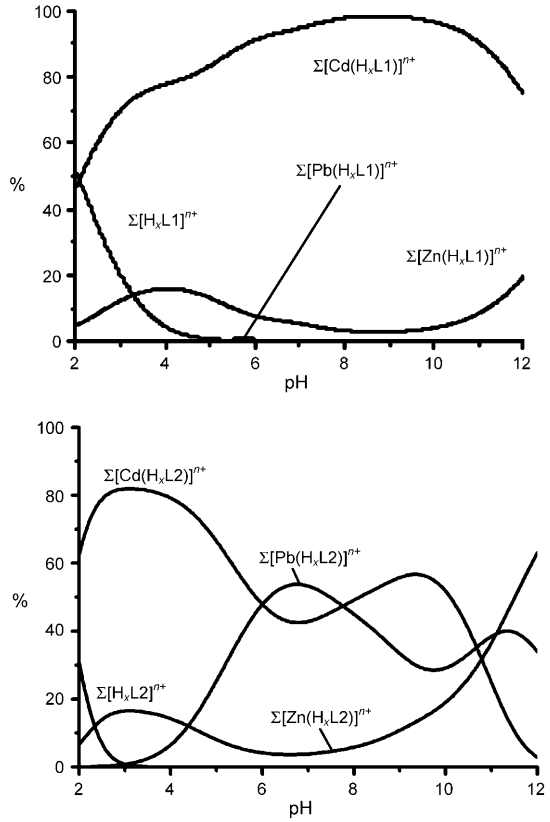

Figure 8. Overall percentages of the L1 (top) and L2 (bottom) complexed species with Zn^{II}, Cd^{II} and Pb^{II} as a function of pH in competitive systems containing Zn^{II}, Cd^{II} and Pb^{II} and L1 or L2 in equimolecular ratio ($[L1]=[L2]=[Zn^{II}]=[Cd^{II}]=[Pb^{II}]=1\times10^{-3}$ M). $\Sigma[M(H_xL)]^{(x-1)+}=[ML]^{2+}+[M(HL)]^{3+}+[M(H_2L)]^{4+}+[M(H_3L)]^{5+}+[M\{(OH)L\}]^{+}+[M\{(OH)_2L\}]$ with L = L1 or L2 and M = Zn, Cd or Pb.

mensional and stereochemical matching between Cd^{II} and this tetradentate coordination site, which possesses the optimal dimension and conformation to host Cd^{II}. This suggestion is supported, once again, by the crystallographic analysis of the $[M(HL1)]^{3+}$ complexes (M = Zn^{II}, Cd^{II} and Pb^{II}) in the solid state. In fact, while Cd^{II} forms four strong Cd–N bonds, Zn^{II} shows weaker M^{II}–N interactions and Pb^{II} features a strongly distorted coordination environment, with two of four bond lengths being remarkably longer.

To verify the presence of a tetradentate cavity well suited to host Cd^{II} that is also in non-protonated complexes, we optimised the $[ML1(H_2O)]^{2+}$ species within the density functional theory (DFT) framework. For all complexes, we used as starting coordinates those derived from the crystal structures of the protonated complexes, by removing the acidic protons and replacing the halogen ion with a water molecule. In fact, halogen ions are generally weakly bound by the present metal cations and therefore they can be easily replaced by a water molecule in aqueous solution. The obtained M–N (M = Zn, Cd or Pb) distances and complete geometries are reported in Table 5 and Figure 9, respectively. Similarly to the crystal structures of the protonated complexes, the metal cations are unequivocally coordinated by

Table 5. M–X (M = Zn, Cd and Pb; X = N, O) distances computed at the B3LYP level for the $[ML1(H_2O)]^{2+}$ complexes.

Complex	M–N1	M–N2	M–N3	M–N6	M–N4	M–N5	M–O
$[ZnL1(H_2O)]^{2+}$	2.118	2.144	2.196	2.112	4.803	3.226	2.065
$[CdL1(H_2O)]^{2+}$	2.342	2.351	2.319	2.279	4.372	3.552	2.251
$[PbL1(H_2O)]^{2+}$	2.507	2.507	2.563	2.564	4.543	4.543	2.313

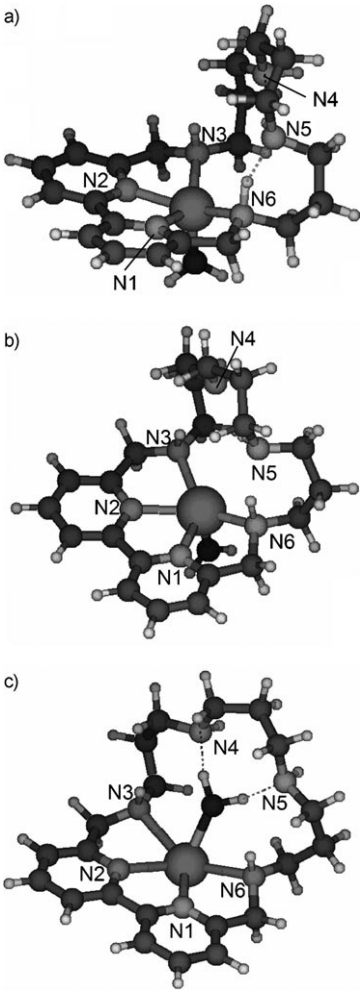

Figure 9. Optimised geometries computed at the B3LYP level for $[ML1(H_2O)]^{2+}$ complexes: a) M = Zn, b) M = Cd, c) M = Pb.

the dipyridine nitrogen atoms and by the adjacent benzylic amine donors, whereas the central amine groups of the aliphatic chain do not show interactions with the metals. The data in Table 5 point out that the most favourable stereochemical matching is found for the Cd^{II} ion. In this case, the L1 ligand acts as a perfect tetradentate ligand. In fact, three of the four closest Cd–N distances are perfectly in agreement with the Cd–N distances generally observed in Cd^{II} complexes with polyaza ligands. The short Cd–N6 should be induced by the non-symmetric L1 folding through the hydrogen bond between the N6 proton and N5. The $[ZnL1(H_2O)]^{2+}$ geometry instead presents fairly longer distances than those usually found in Zn^{II} complexes with polyamine

ligands (mean value 2.087(1) Å, see above), confirming the Zn^{II} ion to be too small to fit into the tetradentate binding site of L1. Similarly to $[CdL1(H_2O)]^{2+}$, the Zn–N6 bond is the shortest one, probably due to the formation of a hydrogen bond between the N6 proton and N5. The $[PbL1(H_2O)]^{2+}$ cation is characterised by a water molecule interacting through hydrogen bonding with the amine groups not involved in metal coordination. Similarly to the crystal structure of $[Pb(H_2L1)Br]^{3+}$, the metal cation is shifted in the opposite direction with respect to the apical position occupied by the water molecule. The two dipyridine nitrogen atoms interact with the metal at very short distances, whereas the two benzylic amine groups are coordinated more weakly. These structural features suggest a not optimal fitting of Pb^{II} within the tetradendate binding site of L1.

Fluorimetric chemosensing of metal cations with L1 and L2: The chemosensing ability of L1 and L2 was studied by means of spectrofluorimetric measurements on aqueous solutions containing the ligand and the selected metal ion in equimolecular ratio at different pH values. In fact, both ligands present a marked pH dependence of their emission spectra. In the case of L1, the emission of the ligand is completely quenched from slightly acidic to alkaline pH values in the presence of Cu^{II} or Pb^{II}. Superimposition of the distribution diagram of the Cu^{II} or Pb^{II} complexes with the maximum of the emission intensity of dipyridine at 345 nm at different pH values clearly shows that the fluorescence quenching is simply due to the formation of the metal complexes (see Figure 10a for Pb^{II}), as generally observed for complexation of paramagnetic ions, such as Cu^{II}, or heavy metal cations, such as Pb^{II}. A different behaviour is observed in the case of Zn^{II} and Cd^{II}, in which a less common pH dependence of the emission spectra is observed. As shown in Figure 10b and c for Cd^{II}, the fluorescence emission displays an OFF–ON–OFF pH profile, with a maximum of the emission intensity at pH 6.2. Figure 10c points out that, among the different complexes present in solution, only the protonated complexes $[Cd(H_xL1)]^{(x+2)+}$ ($x=1$–3) are emissive, whereas $[CdL1]^{2+}$ and its hydroxo derivatives do not show any fluorescence emission. This behaviour, which is also found in the case of the Zn^{II} complexes (see the Supporting Information, Figure S4) can be interpreted in consideration of the fact that the $[ZnL1]^{2+}$ and $[CdL1]^{2+}$ complexes are characterised by the central amine groups of the aliphatic chain not involved or weakly involved in metal coordination (Scheme 2), which may quench the emission of the complex thanks to a PET process involving their lone pairs. As a consequence, the $[ML1]^{2+}$ complexes and their hydroxo derivatives, formed in the alkaline pH region, are not emissive. Protonation of the complexes in the pH range 4–8 takes place on these unbound amine groups (Scheme 2). Binding of a couple of protons or of a single acidic proton, which can be shared by the two central amine groups of the aliphatic chain through hydrogen bonding, can inhibit the PET process, renewing the fluorescence emission of the Zn^{II} and Cd^{II} complexes. Finally, the decrease of the emission observed below pH 4 is simply due to complex decomposition, which affords the free ligand in its tetraprotonated form ($[H_4L1]^{4+}$), an almost non-emissive species. The emissive characteristics of the Zn^{II} and Cd^{II} protonated complexes are also confirmed by the fluorescence emission spectra of $[Zn(HL1)Br][ClO_4]_2$ and $[Cd(HL1)Br][ClO_4]_2$ solid compounds dissolved in anhydrous CH_3CN (see the Supporting Information, Figure S5). In fact, both compounds display a marked fluorescence emission, with a maximum of the intensity at 352 nm, slightly redshifted with respect to the

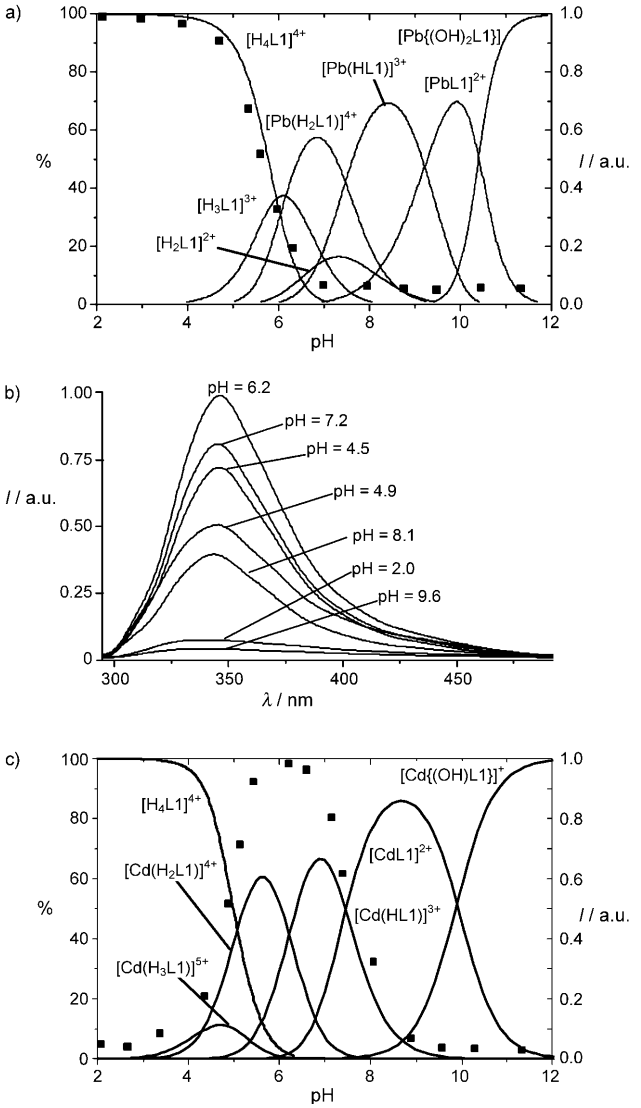

Figure 10. a) Fluorescence emission intensity at 345 nm (■, right *y* axis) as a function of pH compared to the distribution curves of the complexes (——, left *y* axis) for a system containing L1 and Pb^{II} in 1:1 molar ratio ($[L1]=[Pb^{II}]=1\times10^{-5}$ M, $\lambda_{exc}=298$ nm, 298 K, 0.1 M NMe_4NO_3); b) selected fluorescence emission spectra of L1 in the presence of 1 equiv of Cd^{II}; c) fluorescence emission intensity at 345 nm (■, right *y* axis) as a function of pH compared to the distribution curves of the complexes (——, left *y* axis) for a system containing L1 and Cd^{II} in 1:1 molar ratio ($[L1]=[Cd^{II}]=1\times10^{-5}$ M, 298 K, $\lambda_{exc}=298$ nm, 0.1 M NMe_4NO_3).

spectra in aqueous solutions. Conversely, the $[Cu(HL1)(ClO_4)][ClO_4]_2 \cdot H_2O$ complex does not give any emission enhancement.

Of note, addition of increasing amounts of Zn^{II} or Cd^{II} to an aqueous solution of L1, buffered at pH 6.5, leads to a linear increase of the fluorescence emission intensity of dipyridine at 345 nm up to 0.8:1 (in the case of Zn^{II}) or 1:1 (in the case of Cd^{II}) metal to ligand molar ratio (see the Supporting Information, Figure S6). The emission intensity achieves a constant value for molar ratios greater than 1.2 in the case of Cd^{II} or 1.4 in the case of Zn^{II}. These data not only confirm that L1 forms rather stable 1:1 metal chelates with Zn^{II} and Cd^{II}, but also indicate that the receptor is able to ratiometrically sense these metal cations, thanks to chelation-induced enhancement of fluorescence. Furthermore, a competitive experiment carried out by adding increasing amounts of Pb^{II} to a solution containing Cd^{II} and L1 at pH 6.5 in equimolecular ratio shows that the fluorescence emission intensity at 345 nm of the Cd^{II} complex is only slightly affected by the presence of more than 1 equiv of Pb^{II} (for instance, only a 5% reduction of the intensity is observed in the presence of 3 equiv of Pb^{II}; see the Supporting Information Figure S7), that is, the Cd^{II} complex is preferentially formed in high percentages, even in the presence of a large excess of Pb^{II}. Conversely, the same experiment carried out on solutions containing L1 and Zn^{II} in 1:1 molar ratio show an 18% decrease of the emission of the Zn^{II} complex in the presence of only 1 equiv of Pb^{II}. These results point out that the stability of the complexes decreases in the order $Cd^{II} > Zn^{II} > Pb^{II}$, confirming, at least qualitatively, the selectivity pattern deduced from the potentiometric measurements (Figure 8, top). Actually, the ability to selectively bind Cd^{II} over Zn^{II} and Pb^{II}, and to give fluorescent Zn^{II} or Cd^{II} complexes in a narrow pH range represent peculiar features of this receptor.

The complexes with L2 are characterised by different pH dependence. In fact, all the metal complexes, including those with Zn^{II} and Cd^{II}, do not show florescence emission all over the pH range investigated; unlike L1, the Zn^{II} and Cd^{II} protonated complexes $[M(HL2)]^{3+}$ and $[M(H_2L2)]^{4+}$, which are the predominant species in solution in the pH range 4–7 (see Figure 11 for Cd^{II} and the Supporting Information, Figure S8), are not emissive. Whereas the lack of emission of the Cu^{II} and Pb^{II} complexes with L2 can be related, once again, to the paramagnetic or heavy nature of the metal cation, the different emission properties of the protonated Zn^{II} and Cd^{II} complexes with L2 with respect to those with L1 is probably due to the different structural characteristics of the complexes. Differently from L1, the L2 complexes with Zn^{II} or Cd^{II} are characterised by a benzylic amine group not bound or weakly bound to the metal cations. This amine group is less basic than the central amine groups of the aliphatic chain; this suggests that in the $[M(HL2)]^{3+}$ and $[M(H_2L2)]^{4+}$ complexes the unbound benzylic amine group is not involved in proton binding. As already observed in the case of the protonation of the ligand alone, this amine group, positioned at a short distance from the fluorophore, can behave as an efficient quencher of the fluorescence emission of phenanthroline.

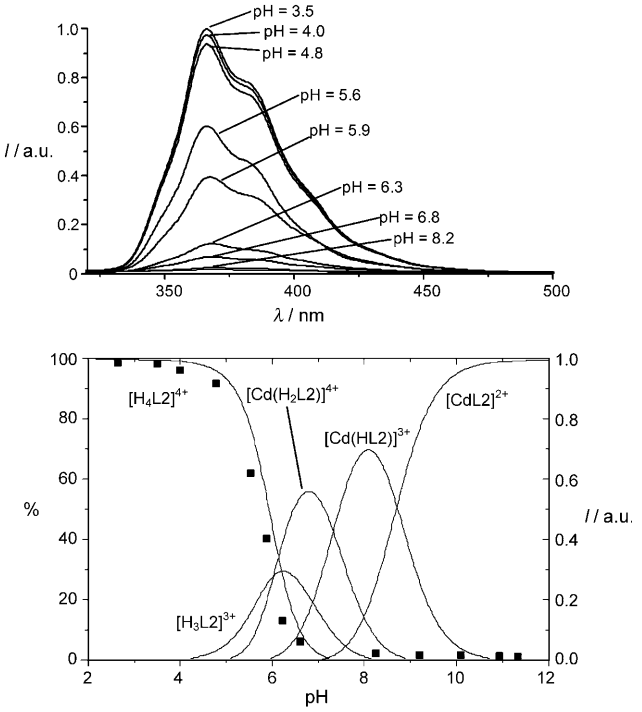

Figure 11. Top: Selected fluorescence emission spectra of L2 in the presence of 1 equiv of Cd^{II}. Bottom: Fluorescence emission intensity at 370 nm (■, right *y* axis) as a function of pH compared to the distribution curves of the complexes (——, left *y* axis) for a system containing L2 and Cd^{II} in 1:1 molar ratio ($[L2] = [Cd^{II}] = 5 \times 10^{-6}$ M, $\lambda_{exc} = 280$ nm, 298 K, 0.1 M NMe_4NO_3).

Conclusion

This study shows that subtle structural parameters can determine the selectivity properties of ligands as well as the fluorescence emission of their complexes. The coupling within the same cyclic structure of a 2,2′-dipyridine unit and an aliphatic tetramine moiety characterised by propylenic spacers between the nitrogen donors gives rise to a ligand able to selectively coordinate Cd^{II} over Zn^{II} and Pb^{II}. This characteristic is due to the presence of a tetradentate cavity with the optimal dimension to host the Cd^{II} ion. Of note, this coordinative site is composed of the less basic heteroaromatic and benzylic nitrogen atoms, whereas the most basic amine groups, located in the middle of the aliphatic chain, are not involved in metal binding and can easily protonate at neutral pH. The simple replacement of dipyridine with phenanthroline, a heteroaromatic unit with a donor ability almost equal to that of dipyridine but more rigid, leads to loss of selectivity. In fact, the rigidity of phenanthroline does not allow the simultaneous involvement of both the heteroaromatic nitrogen atoms and the adjacent benzylic amine groups and the consequent formation of a tetradentate binding site for metal cations. This slight structural difference

also determines the fluorescence emission properties of the Zn^{II} and Cd^{II} complexes. Whereas the dipyridine-containing ligand gives fluorescent protonated complexes at neutral pH, due to the involvement of all nitrogen atoms in metal or proton binding, the phenanthroline-based analogue forms non-emissive complexes at any pH value. In fact, in the L2 complexes, the presence of an unbound benzylic amine group close to the fluorophore can efficiently quench the fluorescent emission of phenanthroline through a PET process.

Experimental Section

Synthesis of ligands and their metal complexes: L2 was prepared as previously reported.[36] Crystals of $[(H_{4.5}L2)(H_2O)_{0.5}Cl_{0.5}][ClO_4]_4\cdot 2H_2O$ suitable for X-ray analysis were obtained in 27% yield by slow evaporation of an HCl (0.1 M) aqueous solution of L2 (0.01 M) in the presence of a tenfold excess of $NaClO_4$. L1 was synthesised by using a modification of the Richmam and Atkins procedure.[37] Reaction of 1,5,9,13-tetratosyl-1,5,9,13-tetraazatridecane (**1**)[36] with 6,6′-bis(bromomethyl)-2,2′-bipyridine[38] (**2**) afforded the tosylated macrocycle (**3**), which was then deprotected in a CH_3COOH/HBr mixture.

6,6′-(2,6,10,14-Tetratosyl-2,6,10,14-tetraaza[15])(3,3′)-2,2′-bipyridylophane (3): A suspension of **2** (940 mg, 2.75 mmol) in dry acetonitrile (250 mL) was added, over a period of 4 h, to a stirred suspension of **1** (2.0 g, 2.5 mmol) and K_2CO_3 (3.45 g, 25 mmol) in dry acetonitrile (250 mL) at reflux, under a nitrogen atmosphere. At the end of the addition, the mixture was kept under stirring at reflux for an additional 2 h. The suspension was filtered on Celite, washed with acetonitrile, and the resulting solution was evaporated under reduced pressure to obtain a crude solid, which was purified by column chromatography on neutral aluminium oxide by using a petroleum ether/ethyl acetate 1:2 mixture as eluent. Pure compound **3** was obtained as a white solid (862 mg, 35% yield). ^{1}H NMR (300 MHz, [D]$CHCl_3$, 25 °C, TMS): $\delta = 8.18$ (d, $J = 7.8$ Hz, 2H), 7.70 (d, $J = 7.8$ Hz, 2H), 7.60 (d, $J = 8.2$ Hz, 4H), 7.48 (d, $J = 7.0$ Hz, 2H), 7.40 (d, $J = 8.2$ Hz, 4H), 7.25 (d, $J = 8.3$ Hz, 4H), 7.08 (d, $J = 8.3$ Hz, 4H), 4.27 (s, 4H), 2.95–2.90 (m, 6H), 2.77–2.71 (m, 6H), 2.34 (s, 6H), 2.26 (s, 6H), 1.34–1.26 ppm (m, 6H); ^{13}C NMR (100 MHz, [D]$CHCl_3$, 25 °C, TMS): $\delta = 159.0$, 157.2, 143.7–143.3, 136.1–135.0, 137.4, 129.7–129.5, 127.1–126.8, 120.5, 119.3, 52.5, 48.3, 47.5, 46.9, 45.2, 28.7, 28.0, 21.3 ppm.

6,6′-(2,6,10,14-Tetraaza[15])-2,2′-bipyridylophane pentahydrobromide (L1·5HBr): Compound **3** (985 mg, 1 mmol) and phenol (7.5 g, 80 mmol) were dissolved in a HBr/AcOH 33% mixture (100 mL); the solution was kept under stirring at 90 °C for 20 h, until a white precipitate was formed. The reaction mixture was cooled to room temperature and then CH_2Cl_2 (100 mL) was added to complete the precipitation and the suspension was stirred for an additional 1 h. The solid residue was filtered and washed several times with CH_2Cl_2. The hydrobromide salt was then recrystallised from a EtOH/water 3:1 (v/v) mixture, filtered and dried under vacuum at 40 °C overnight. Yield: 470 mg, 61%; ^{1}H NMR (300 MHz, $[D_2]H_2O$, pH 4.5, 25 °C, DSS): $\delta = 8.27$ (d, $J = 7.0$ Hz, 2H), 8.12 (d, $J = 7.8$ Hz, 2H), 7.64 (d, $J = 7.6$ Hz, 2H), 4.56 (s, 4H), 3.33 (t, $J = 7.6$ Hz, 4H), 3.21 (t, $J = 5.4$, 4H), 3.05 (t, $J = 7.2$ Hz, 4H), 2.15 (t, $J = 7.0$ Hz, 4H), 2.01 ppm (t, $J = 7.1$ Hz, 2H); ^{13}C NMR (75 MHz, $[D_2]H_2O$, pH 4.5, 25 °C, DSS): $\delta = 154.4$, 150.3, 140.3, 125.1, 123.1, 50.9, 44.5, 43.3, 43.2, 22.1, 21.3 ppm; MS (ESI): m/z (%): 368.30 (100) $[M^+ + H]$, 184.6 (100) $[M^{2+} + 2H]$; elemental analysis calcd (%) for $C_{21}H_{32}N_6\cdot 5HBr$ ($M_r = 773.08$): C 32.63, H 4.82, N 10.87; found: C 32.41, H 5.03, N 10.69.

$[Cu(HL1)(ClO_4)][ClO_4]_2\cdot H_2O$ (a): $Cu(ClO_4)_2\cdot 6H_2O$ (14.8 mg, 0.04 mmol) was added to a solution of L1·5HBr (30 mg, 0.04 mmol) in water (10 mL). The pH of the solution was adjusted to 5 by slow addition of a few drops of 0.1 M NaOH. The solution was then stirred for 30 min and then $NaClO_4\cdot H_2O$ (100 mg) was added. Crystals of the complex suitable for X-ray analysis were obtained by slow evaporation at room temperature of the resulting solution. Yield: 19.3 mg (64.3%); elemental analysis calcd (%) for $C_{21}H_{35}N_6CuCl_3O_{13}$ ($M_r = 749.45$): C 33.66, H 4.71, N 11.21; found: C 33.4, H 4.8, N 11.2.

$[Zn(HL1)Br][ClO_4]_2$ (b): Crystals suitable for X-ray analysis of this complex were prepared from $Zn(ClO_4)_2\cdot 6H_2O$ (14.9 mg, 0.04 mmol) and L1·5HBr (30 mg, 0.04 mmol) by using a procedure similar to that used for **a**, adjusting the pH of the solution to 6. Yield: 22.1 mg (77.5%); elemental analysis calcd (%) for $C_{21}H_{33}N_6ZnBrCl_2O_8$ ($M_r = 712.71$): C 35.34, H 4.66, N 11.77; found: C 35.4, H 4.7, N 11.7.

$[Cd(HL1)Br][ClO_4]_2$ (c): Crystals suitable for X-ray analysis of this complex were prepared from $CdBr_2\cdot 4H_2O$ (14.8 mg, 0.04 mmol) and L1·5HBr (30 mg, 0.04 mmol) by using the same procedure used for complex **a**. Yield: 22.0 mg (72.4%); elemental analysis calcd (%) for $C_{21}H_{33}N_6CdBrCl_2O_8$ ($M_r = 760.75$): C 33.16, H 4.37, N 11.05; found: C 33.3, H 4.5, N 11.0.

$[Pb(H_2L1)Br][ClO_4]_3\cdot H_2O$ (d): Crystals suitable for X-ray analysis of this complex were prepared from $PbBr_2\cdot 3H_2O$ (16.8 mg, 0.04 mmol) and L1·5HBr (30 mg, 0.04 mmol) by using the same procedure used for complex **a**. Yield: 25.5 mg (65.4%); elemental analysis calcd (%) for $C_{21}H_{36}N_6PbBrCl_3O_{12}$ ($M_r = 947.12$): C 25.90, H 3.73, N 8.63; found: C 25.8, H: 3.8, N 8.6.

Caution! Perchlorate salts of organic ligands and their metal complexes are potentially explosive; these compounds must be handled with great care.

$[Pb(HL2)Br][PF_6]_{1.5}[NO_3]_{0.5}\cdot H_2O$ (e): $Pb(NO_3)_2\cdot 3H_2O$ (15.4 mg, 0.04 mmol) was added to a solution of L2·4HBr (28.6 mg, 0.04 mmol) in water (10 mL). The pH of the solution was adjusted to 6 by slow addition of a few drops of NaOH (0.1 M). The solution was then stirred for 30 min and then KPF_6 (40 mg) was added. Crystals of the complex suitable for X-ray analysis were obtained by slow evaporation at room temperature of the resulting solution. Yield: 18.2 mg (60.7%); elemental analysis calcd (%) for $PbC_{23}H_{35}N_{6.5}BrP_{1.5}F_9O_{2.5}$ ($M_r = 749.45$): C 29.17, H 3.72, N 9.61; found: C 29.3, H 3.7, N 9.6.

Potentiometric measurements: Equilibrium constants for protonation and complexation reactions with L were determined by pH-metric measurements at (298.1 ± 0.1) K in 0.1 M NMe_4NO_3, by using equipment and procedures[39] that have been already described. Ligand and metal ion concentrations of $(1–2)\times 10^{-3}$ M were employed in the potentiometric measurements, with varying of the metal to ligand molar ratio from 0.5:1 to 2:1. Three titrations (about 100 data points for each one) were performed in the pH range 2–12. The computer program HYPERQUAD[40] was used to calculate equilibrium constants from electromotive force (emf) values.

Spectrophotometric and spectrofluorimetric measurements: Absorption spectra were recorded on a Perkin–Elmer Lambda 25 spectrophotometer. Fluorescence emission spectra were collected on a Perkin–Elmer LS55 spectrofluorimeter. In the measurements carried out at different pH values, HNO_3 and NaOH were used to adjust the pH values that were measured on a Metrohm 713 pH meter. Tris(hydroxymethyl)aminomethane (TRIS) buffer (1 mM) was used in the titrations performed at pH 6.5. In the competition experiments, successive readings of the emission intensity were carried out after each addition of Pb^{II} to ensure that the equilibrium was reached.

NMR spectroscopy: ^{1}H (300 MHz) and ^{13}C (75 MHz) NMR spectra of samples in $CDCl_3$ and D_2O at different pH values were recorded at 298 K on a Varian Gemini 300 spectrometer. To adjust the pD, small amounts of NaOD (0.01 M) and DCl were added to the solution containing L1. The pH was calculated from the measured pD values by using the following formula: pH = pD − 0.40.[41] ^{1}H-^{1}H and ^{1}H-^{13}C 2D correlation experiments were performed to assign the ^{1}H NMR spectroscopic signals.

Crystal structure analyses: Data for the X-ray structural analyses of $[(H_{4.5}L2)(H_2O)_{0.5}Cl_{0.5}][ClO_4]_4\cdot 2H_2O$, $[Cu(HL1)(ClO_4)][ClO_4]_2\cdot H_2O$ (**a**), $[Zn(HL1)Br][ClO_4]_2$ (**b**), $[Cd(HL1)Br][ClO_4]_2$ (**c**), $[Pb(H_2L1)Br][ClO_4]_3\cdot H_2O$ (**d**) and $[Pb(HL2)Br][PF_6]_{1.5}[NO_3]_{0.5}\cdot H_2O$ (**e**) were collected using an Oxford Diffraction Xcalibur3 diffractometer equipped with CCD area detector and graphite monochromated $Mo_{K\alpha}$ radiation. Data

Table 6. Crystal data and structure refinement for $[(H_{4.5}L2)(H_2O)_{0.5}Cl_{0.5}][ClO_4]_4\cdot 2H_2O$, $[Cu(HL1)(ClO_4)][ClO_4]_2\cdot H_2O$ (**a**), $[Zn(HL1)Br][ClO_4]_2$ (**b**), $[Cd(HL1)Br][ClO_4]_2$ (**c**), $[Pb(H_2L1)Br][ClO_4]_3\cdot H_2O$ (**d**) and $[Pb(HL2)Br][PF_6]_{1.5}[NO_3]_{0.5}\cdot H_2O$ (**e**).

	$[(H_{4.5}L2)(H_2O)_{0.5}Cl_{0.5}][ClO_4]_4\cdot 2H_2O$	**a**	**b**	**c**	**d**	**e**
formula	$C_{23}H_{41.5}Cl_{4.5}N_6O_{18.5}$	$C_{21}H_{35}Cl_3CuN_6O_{13}$	$C_{21}H_{33}BrCl_2N_6O_8Zn$	$C_{21}H_{33}BrCdCl_2N_6O_8$	$C_{21}H_{36}BrCl_3N_6O_{13}Pb$	$C_{23}H_{35}BrF_9N_{6.5}O_{2.5}P_{1.5}Pb$
M_r	857.65	749.44	713.71	760.74	974.01	947.13
crystal system	triclinic	triclinic	triclinic	triclinic	monoclinic	orthorhombic
space group	$P\bar{1}$	$P\bar{1}$	$P\bar{1}$	$P\bar{1}$	$P2_1/a$	$Pcca$
crystal size [mm^3]	$0.25\times0.2\times0.2$	$0.3\times0.2\times0.1$	$0.4\times0.3\times0.1$	$0.2\times0.1\times0.1$	$0.3\times0.3\times0.2$	$0.3\times0.25\times0.1$
a [Å]	7.540(5)	8.335(1)	8.262(3)	8.503(3)	14.161(1)	35.219(2)
b [Å]	12.277(2)	13.020(2)	13.446(4)	13.253(4)	11.3706(8)	13.5409(6)
c [Å]	19.118(7)	15.066(2)	13.537(4)	13.794(3)	20.586(2)	13.0922(7)
α [°]	83.97(1)	73.93(1)	101.51(2)	101.6(2)	90	90
β [°]	79.31(2)	78.90(1)	100.12(3)	102.7(3)	97.520(7)	90
γ [°]	84.28(1)	84.34(1)	101.09(2)	102.4(3)	90	90
V [Å^3]	1724(1)	1539.9(4)	1409.8(8)	1429.8(7)	3286.2(5)	3286.2(5)
Z	2	2	2	2	4	4
T [K]	298	298	298	298	298	298
λ [Å]	0.71069	0.71069	0.71069	0.71069	0.71069	0.71069
ρ_{calcd} [mg m^{-3}]	1.653	1.616	1.681	1.767	1.969	2.015
μ ($Mo_{K\alpha}$) [mm^{-1}]	0.471	1.041	2.533	2.403	6.663	6.852
F(000)	892	774	728	764	1904	3672
θ_{max} [°]	22	23.25	23.25	28.52	23.81	23.25
total reflns	18739	9283	11191	14295	14970	16549
unique reflns	5855	4161	3986	6034	5012	4462
(R_{int})	(0.0243)	(0.0483)	(0.0804)	(0.0538)	(0.0555)	(0.0681)
observed reflns ($I>2\sigma(I)$)	4339	2263	2296	4319	2995	2361
parameters	478	442	388	360	406	403
GOF	1.075	0.934	1.121	1.097	0.954	0.922
wR_2[a] (all data)	0.1285	0.1360	0.2455	0.2048	0.1056	0.1316
R_1[b] ($I>2\sigma(I)$)	0.0423	0.0528	0.0880	0.0635	0.0451	0.0492

[a] $R_1=\Sigma||F_o|-|F_c||/\Sigma|F_o|$. [b] $wR_2=[\Sigma w(F_o^2-F_c^2)^2/\Sigma wF_o^4]^{1/2}$.

collection was performed using a ω scan with the CrysAlis CCD program.[42] Data reduction was carried out with the CrysAlis Red program,[43] and an empirical absorption correction was applied using spherical harmonics, implemented with the SCALE3 ABSPACK scaling algorithm.[43] Structures were solved by direct methods (SIR2004)[44] and refined against F^2 by using SHELXL-97,[45] with non-hydrogen atoms anisotropic and hydrogen atoms in riding mode. A summary of data collection and structure refinement is reported in Table 6. In $[(H_{4.5}L2)(H_2O)_{0.5}Cl_{0.5}][ClO_4]_4\cdot 2H_2O$, the water oxygen O3 and the chloride Cl5, enclosed in the macrocyclic cavity, share almost the same position and have been refined with partial occupational parameters (0.5). Attempts performed to refine the structure in the $P1$ space group, considering a doubled content of the asymmetric unit, failed; in **a** the H1, H2 and H4 hydrogen atoms, bound to the N4 and N5 secondary nitrogen atoms, have been localised in the ΔF map, introduced in the calculation and isotropically refined with a fixed thermal parameter ($U=0.05$ Å^2); in **b**, the acidic proton has not been localised in the ΔF map, and has been introduced in a calculated position with a partial population parameter (0.5) on the secondary N4 and N5 nitrogen atoms. Disorder has been found for one of the perchlorate anions, the oxygen atoms of which have been found distributed over two different positions with equal occupational factor (O41, O42, O43, O44 and O41′, O42′, O43′, O44′); in **c**, the H1 and H2 hydrogen atoms, bound to the N4 secondary nitrogen, have been localised in the ΔF map, introduced in the calculation and isotropically refined; in **d** the hydrogen atoms belonging to the water solvent molecule have not been localised in the ΔF map and not introduced in the calculation; in **e** one of the PF_6^- anion and the nitrate anion lie on crystallographic C_2 axes and are consequently only partially contained in the asymmetric unit. The acidic proton has not been localised in the ΔF map, and has been introduced in calculated position on the secondary N4 and N5 nitrogen atoms with a partial population parameter (0.5). CCDC-716578 ($[(H_{4.5}L2)(H_2O)_{0.5}Cl_{0.5}][ClO_4]_4\cdot 2H_2O$), 716577 (**a**), 716581 (**b**), 716576 (**c**), 716579 (**d**) and 716580 (**e**) contain the supplementary crystallographic data for this paper. These data can be obtained free of charge from the Cambridge Crystallographic Data Centre via www.ccdc.cam.ac.uk/data_request/cif.

Computational details: GAMESS US software package[46] was used throughout all the calculations. The default thresholds were used for all the optimisations. Hay–Wadt pseudopotentials and basis sets[47] were used for Zn^{II} and Cd^{II} complexes. SBK pseudopotentials and basis sets[48] were used for the Pb^{II} complex. The B3LYP functional[49] was used throughout all the calculations.

Acknowledgements

Financial support of MIUR (PRIN 2007) is gratefully acknowledged.

[1] Selected reviews: a) V. Balzani, G. Bergamini, P. Ceroni, *Coord. Chem. Rev.* **2008**, *252*, 2456–2469; b) L. Prodi, M. Montalti, N. Zaccheroni, L. S. Dolci in *Topics in Fluorescence Spectroscopy, Vol. 9* (Eds C. D. Geddes, J. R. Lakowicz), Springer, New York, **2005**, pp. 1–57; c) L. Fabbrizzi, M. Licchelli, G. Rabaioli, A. Taglietti, *Coord. Chem. Rev.* **2000**, *205*, 85–108; d) B. Valeur, I. Leray, *Coord. Chem. Rev.* **2000**, *205*, 3–40; e) V. Amendola, M. Bonizzoni, D. Esteban-Gomez, L. Fabbrizzi, M. Licchelli, F. Sancenon, A. Taglietti, *Coord. Chem. Rev.* **2006**, *250*, 1451–1470; f) R. Martinez-Mañez, F. Sancenon, *Chem. Rev.* **2003**, *103*, 4419–4476; g) B. Valeur, *Molecular Fluorescence*, Wiley-VCH, Weinheim, **2002**; h) A. P. de Silva,

H. Q. N. Gunaratne, T. Gunnlauson, A. J. M. Huxley, C. P. McCoy, J. T. Rademacher, T. E. Rice, *Chem. Rev.* **1997**, *97*, 1515–1566; i) J. L. Sessler, J. M. Davis, *Acc. Chem. Res.* **2001**, *34*, 989–997; j) P. D. Beer, P. A. Gale, *Angew. Chem.* **2001**, *113*, 502–532; *Angew. Chem. Int. Ed.* **2001**, *40*, 486–516; k) M. D. Best, S. L. Tobey, E. V. Anslyn, *Coord. Chem. Rev.* **2003**, *240*, 3–15; l) L. Prodi, *New J. Chem.* **2005**, *29*, 20–31; m) F. Pina, M. A. Bernardo, E. Garcia-España, *Eur. J. Inorg. Chem.* **2000**, 2143–2157; n) A. J. Parola, J. C. Lima, C. Lodeiro, F. Pina in *Fluorescence of Supermolecules, Polymers, and Nanosystems, Springer Series on Fluorescence, Vol. 4* (Ed.: M. N. Berberan-Santos), Springer, Berlin, **2008**, pp. 117–149;o) V. Amendola, L. Fabbrizzi, F. Foti, M. Licchelli, C. Mangano, P. Pallavicini, A. Poggi, D. Sacchi, A. Taglietti, *Coord. Chem. Rev.* **2006**, *250*, 273–299; p) A. Bencini, M. A. Bernardo, A. Bianchi, E. Garcia-España, C. Giorgi, S. Luis, F. Pina, B. Valtancoli in *Advances in Supramolecular Chemistry, Vol. 8* (Ed.: G. W. Gokel), Cerberus Press, Miami, **2002**, pp. 79–130.

[2] a) Z. Wang, M. A. Palacios, P. Anzenbacher, *Anal. Chem.* **2008**, *80*, 7451–7459; b) M. A. Palacios, Z. Wang, V. A. Montes, G. V. Zyryanov, P. Anzenbacher, *J. Am. Chem. Soc.* **2008**, *130*, 10307–10314.

[3] a) M. Arduini, F. Mancin, P. Tecilla, U. Tonellato, *Langmuir* **2007**, *23*, 8632–8636; b) P. Teolato, E. Rampazzo, M. Arduini, F. Mancin, P. Tecilla, U. Tonellato, *Chem. Eur. J.* **2007**, *13*, 2238–2245; c) F. Mancin, E. Rampazzo, P. Tecilla, U. Tonellato, *Chem. Eur. J.* **2006**, *12*, 1844–1854.

[4] I. Stoll, J. Eberhard, R. Brodbeck, W. Eisfeld, J. Mattay, *Chem. Eur. J.* **2008**, *14*, 1155–1163.

[5] J. Tolosa, A. J. Zucchero, U. H. F. Bunz, *J. Am. Chem. Soc.* **2008**, *130*, 6498–6506.

[6] B. Garcia-Acosta, R. Martinez-Manez, F. Sancenon, J. Soto, K. Rurack, M. Spieles, E. Garcia-Breijo, L. Gil, *Inorg. Chem.* **2007**, *46*, 3123–3135.

[7] a) P. Pallavicini, Y. Diaz-Fernandez, F. Foti, C. Mangano, S. Patroni, *Chem. Eur. J.* **2006**, *12*, 178–187; b) Y. Diaz Fernandez, A. Perez Gramatges, V. Amendola, F. Foti, C. Mangano, P. Pallavicini, S. Patroni, *Chem. Commun.* **2004**, 1650–1651.

[8] a) M. C. Aragoni, M. Arca, A. Bencini, A. J. Blake, C. Caltagirone; G. De Filippo, F. A. Devillanova, A. Garau, T. Gelbrich, M. B. Hursthouse, F. Isaia, V. Lippolis, M. Mameli, P. Mariani, B. Valtancoli, C. Wilson, *Inorg. Chem.* **2007**, *46*, 4548–4559, A. Danesi, F. A. Devillanova, A. Garau, T. Gelbrich, F. Isaia, V. Lippolis, M. B. Hursthouse, B. Valtancoli, C. Wilson, *Inorg. Chem.* **2007**, *46*, 8088–8097; b) M. C. Aragoni, M. Arca, A. Bencini, A. J. Blake, C. Caltagirone; G. De Filippo, F. A. Devillanova, A. Garau, T. Gelbrich, M. B. Hursthouse, F. Isaia, V. Lippolis, M. Mameli, P. Mariani, B. Valtancoli, C. Wilson, *Inorg. Chem.* **2007**, *46*, 4548–4559; c) M. C. Aragoni, M. Arca, A. Bencini, A. J. Blake, C. Caltagirone, A. Decortes, F. Demartin, F. A. Devillanova, E. Faggi, L. S. Dolci, A. Garau, F. Isaia, V. Vito, L. Prodi, C. Wilson, B. Valtancoli, N. Zaccheroni, *Dalton Trans.* **2005**, 2994–3004.

[9] a) C. Bazzicalupi, A. Bencini, E. Berni, A. Bianchi, L. Borsari, C. Giorgi, B. Valtancoli, C. Lodeiro, J. C. Lima, A. J. Parola, F. Pina, *Dalton Trans.* **2004**, 591–597; b) C. Bazzicalupi, A. Bencini, A. Bianchi, L. Borsari, A. Danesi, C. Giorgi, C. Lodeiro, P. Mariani, F. Pina, S. Santarelli, A. Tamayo, B. Valtancoli, *Dalton Trans.* **2006**, 4000–4010; c) C. Bazzicalupi, A. Bencini, E. Berni, A. Bianchi, A. Danesi, C. Giorgi, B. Valtancoli, C. Lodeiro, J. C. Lima, F. Pina, A. M. Bernardo, *Inorg. Chem.* **2004**, *43*, 5134–5146; d) C. Lodeiro, A. J. Parola, F. Pina, C. Bazzicalupi, A. Bencini, A. Bianchi, C. Giorgi, A. Masotti, B. Valtancoli, *Inorg. Chem.* **2001**, *40*, 2968–2975; e) A. Bencini, M. A. Bernardo, A. Bianchi, V. Fusi, C. Giorgi, F. Pina, B. Valtancoli, *Eur. J. Inorg. Chem.* **1999**, 1911–1918; f) C. Bazzicalupi, A. Bencini, A. Bianchi, C. Giorgi, V. Fusi, B. Valtancoli, M. A. Bernardo, F. Pina, *Inorg. Chem.* **1999**, *38*, 3806–3813.

[10] a) M. Chadlaoui, B. Abarca, R. Ballesteros, C. Ramirez de Arellano, J. Aguilar, R. Aucejo, E. Garcia-España, *J. Org. Chem.* **2006**, *71*, 9030–9034; b) J. Pina, J. Seixas de Melo, F. Pina, C. Lodeiro, J. C. Lima, A. J. Parola, C. Soriano, M. P. Clares, M. T. Albelda, R. Aucejo, E. Garcia-España, *Inorg. Chem.* **2005**, *44*, 7449–7458; c) J. Alarcón, M. T. Albelda, R. Belda, M. P. Clares, E. Delgado-Pinar, J. C. Frias, E. Garcia-España, J. Gonzalez, C. Soriano, *Dalton Trans.* **2008**, 6530–6538.

[11] D. W. Domaille, E. L. Que, C. J. Chang, *Nat. Chem. Biol.* **2008**, *47*, 168–175.

[12] a) R. M. F. Batista, E. Oliveira, S. P. G. Costa, C. Lodeiro, M. Raposo, *Tetrahedron Lett.* **2008**, *49*, 6575–6578; b) A. Tamayo, B. Pedras, C. Lodeiro, L. Escriche, J. Casabo, J. L. Capelo, B. Covelo, R. Kivekas, R. Sillanpaa, *Inorg. Chem.* **2007**, *46*, 7818–7826.

[13] a) M. Boiocchi, L. Fabbrizzi, M. Licchelli, D. Sacchi, M. Vazquez, C. Zampa, *Chem. Commun.* **2003**, 1812–1813; b) L. Fabbrizzi, F. Foti, M. Licchelli, A. Poggi, *Inorg. Chem.* **2002**, *41*, 4612–4614; c) L. Fabbrizzi, M. Licchelli, F. Mancin, M. Pizzeghello, G. Rabaioli, A. Taglietti, P. Tecilla, U. Tonellato, *Chem. Eur. J.* **2002**, *8*, 94–101; d) M. Di Casa, L. Fabbrizzi, M. Licchelli, A. Poggi, A. Russo, A. Taglietti, *Chem. Commun.* **2001**, 825–826.

[14] a) J. V. Ros-Lis, R. Martinez-Manez, F. Sancenon, J. Soto, M. Spieles, K. Rurack, *Chem. Eur. J.* **2008**, *14*, 10101–10114; b) J. V. Ros-Lis, R. Martinez-Manez, K. Rurack, F. Sancenon, J. Soto, M. Spieles, *Inorg. Chem.* **2004**, *43*, 5183–5185; c) F. Sancenon, R. Martinez-Manez, J. Soto, *Tetrahedron Lett.* **2001**, *42*, 4321–4323; d) M. E. Padilla-Tosta, J. M. Lloris, R. Martinez-Manez, M. D. Marcos, M. A. Miranda, T. Pardo, F. Sancenon, J. Soto, *Eur. J. Inorg. Chem.* **2001**, 1475–1482.

[15] a) J. F. Callan, A. P. de Silva, D. C. Magri, *Tetrahedron* **2005**, *61*, 8551–8588; b) A. P. de Silva, D. B. Fox, A. J. M. Huxley, T. S. Moody, *Coord. Chem. Rev.* **2000**, *205*, 41–57.

[16] a) Z. Dai, J. W. Canary, *New J. Chem.* **2007**, *31*, 1708–1718; b) M. Royzen, A. Durandin, V. G. J. Young, N. E. Geacintov, J. W. Canary, *J. Am. Chem. Soc.* **2006**, *128*, 3854–3855; c) M. Royzen, Z. Dai, J. W. Canary, *J. Am. Chem. Soc.* **2005**, *127*, 1612–1613.

[17] a) X. Zhang, D. Hayes, S. J. Smith, S. Friedle, S. J. Lippard, *J. Am. Chem. Soc.* **2008**, *130*, 15788–15789; b) E. M. Nolan, S. J. Lippard, *J. Am. Chem. Soc.* **2007**, *129*, 5910–5918; c) E. M. Nolan, S. J. Lippard, *Chem. Rev.* **2008**, *108*, 3443–3480; d) C. J. Chang, S. J. Lippard in *Neurodegenerative Diseases and Metal Ions* (Eds.: A. Sigel, H. Sigel, K. O. Sigel), Wiley-VCH, Weinheim, **2006**, pp. 321–370; e) S. C. Burdette, G. K. Grant B. Spingler, R. Y. Tsien, S. J. Lippard, *J. Am. Chem. Soc.* **2001**, *123*, 7831–7841.

[18] G. Farruggia, S. Iotti, L. Prodi, M. Montalti, N. Zaccheroni, P. B. Savage, V. Trapani, P. Sale, F. Wolf, *J. Am. Chem. Soc.* **2006**, *128*, 344–350.

[19] a) W. M. Leevy, S. T. Gammon, H. J. Jiang, J. R. Johnson, D. J. Maxwell, E. N. Jackson, M. Marquez, D. Piwnica-Worms, B. D. Smith, *J. Am. Chem. Soc.* **2006**, *128*, 16476–16477; b) K. M. DiVittorio, W. M. Leevy, E. J. O'Neil, J. R. Johnson, S. Vakulenko, J. D. Morris, K. D. Rosek, N. Serazin, S. Hilkert, S. Hurley, M. Marquez, B. D. Smith, *ChemBioChem* **2008**, *9*, 286–293.

[20] a) M. Soibinet, L. Souchon, I. Leray, B. Valeur, *J. Fluoresc.* **2008**, *18*, 1077–1082; b) V. Souchon, I. Leray, B. Valeur, *Chem. Commun.* **2006**, 4224–4226; c) J. P. Malval, I. Leray, B. Valeur, *New J. Chem.* **2005**, *29*, 1089–1094; d) R. Métivier, I. Leray, V. Bernard, *Chem. Eur. J.* **2004**, *10*, 4480–4490.

[21] a) R. Parkesh, T. C. Lee, T. Gunnlaugsson, *Org. Biomol. Chem.* **2007**, *5*, 310–317; b) T. Gunnlaugsson, T. C. Lee, R. Parkesh, *Tetrahedron* **2004**, *60*, 11239–11249; c) T. Gunnlaugsson, J. P. Leonard, N. S. Murray, *Org. Lett.* **2004**, *6*, 1557–1560; d) T. Gunnlaugsson, T. C. Lee, R. Parkesh, *Org. Lett.* **2003**, *5*, 4065–4068.

[22] a) L. F. Lindoy, *The Chemistry of Macrocyclic Ligand Complexes*, Cambridge University Press, Cambridge, **1989**; b) L. F. Lindoy, *Pure Appl. Chem.* **1997**, *69*, 2179–2186.

[23] J. S. Bradshaw, *Aza-crown Macrocycles*, Wiley, New York, **1993**.

[24] a) K. B. Mertes, J. M. Lehn in *Comprehensive Coordination Chemistry* (Ed.: G. Wilkinson), Pergamon, Oxford, **1987**, pp. 915–1009; b) J. M. Lehn, *Supramolecular Chemistry*, VCH, Weinheim, **1995**.

[25] P. Guerriero, S. Tamburini, P. A. Vigato, *Coord. Chem. Rev.* **1995**, *113*, 17–243.

[26] J. Nelson, V. McKee, G. Morgan, in *Progress in Inorganic Chemistry, Vol. 47* (Ed.: K. D. Karlin), Wiley, New York, **1998**, pp. 167–213.

[27] a) C. Anda, C. Bazzicalupi, A. Bencini, A. Bianchi, P. Fornasari, C. Giorgi, B. Valtancoli, C. Lodeiro, A. J. Parola, F. Pina, *Dalton Trans.* **2003**, 1299–1307; b) C. Bazzicalupi, A. Belusci, A. Bencini, E. Berni, A. Bianchi, S. Ciattini, C. Giorgi, B. Valtancoli, *J. Chem. Soc. Dalton Trans.* **2002**, 2151–2157; c) C. Bazzicalupi, A. Bencini, A. Bianchi, L. Borsari, A. Danesi, C, Giorgi, C. Lodeiro, P. Mariani, F. Pina, S. Santarelli, A. Tamayo, B. Valtancoli, *Dalton Trans.* **2006**, 4000–4010; d) P. Arranz, C. Bazzicalupi, A. Bencini, A. Bianchi, S. Ciattini, P. Fornasari, C. Giorgi, B. Valtancoli, *Inorg. Chem.* **2001**, *40*, 6383–6389; e) D. K. Chand, H.-J. Schneider, A. Bencini, A. Bianchi, C. Giorgi, S. Ciattini, B. Valtancoli, *Chem. Eur. J.* **2000**, *6*, 4001–4008; f) A. Bencini, A. Bianchi, V. Fusi, C. Giorgi, A. Masotti, P. Paoletti, *J. Org. Chem.* **2000**, *65*, 7686; g) C. Bazzicalupi, A. Bencini, V. Fusi, C. Giorgi, P. Paoletti, B. Valtancoli, *J. Chem. Soc. Dalton Trans.* **1999**, 393–400; h) C. Bazzicalupi, A. Bencini, V. Fusi, C. Giorgi, P. Paoletti, B. Valtancoli, *Inorg. Chem.* **1998**, *37*, 941–948.

[28] R. D. Hancock, A. E. Martell, *Chem. Rev.* **1989**, *89*, 1875–1914.

[29] A. Bencini, A. Bianchi, E. Garcia-España, M. Micheloni, J. A. Ramirez, *Coord. Chem. Rev.* **1999**, *188*, 97–156.

[30] R. M Smith, A. E. Martell, NIST Stability Constants Database, Version 4.0, National Institute of Standards and Technology, Washington, **1997**.

[31] C. Bazzicalupi, A. Bencini, E. Berni, A. Bianchi, P. Fornasari, C. Giorgi, C. Marinelli, B. Valtancoli, *Dalton Trans.* **2003**, 2564–2570.

[32] a) N. Armaroli, L. De Cola, V. Balzani, J.-P. Sauvage, C. O. Dietrich-Buchecker, J. M. Kern, *J. Chem. Soc. Faraday Trans.* **1992**, *88*, 553–556; b) J. M. Kern, J.-P. Sauvage, J. L. Weidmann, N. Armaroli, L. Flamigni, P. Ceroni, V. Balzani, *Inorg. Chem.* **1997**, *36*, 5329–5338; c) N. Armaroli, L. De Cola, V. Balzani, J.-P. Sauvage, C. O. Dietrich-Buchecker, J. M. Kern, A. Bailal, *J. Chem. Soc. Dalton Trans.* **1993**, 3241–3247; <lit d>N. Armaroli, P. Ceroni, V. Balzani, J. M. Kern, J.-P. Sauvage, J. L. Weidmann, *J. Chem. Soc. Faraday Trans.* **1997**, *93*, 4145–4150.

[33] a) F. H. Allen, *Acta Crystallogr. Sect. B* **2002**, *58*, 380–388; b) Cambridge Structural Database, Version 5.29, **2007**.

[34] a) R. D. Hancock, M. S. Shaikjee, S. M. Dobson, C. A. Boeyens, *Inorg. Chim. Acta* **1988**, *154*, 229–238; b) V. J. Thom, M. S. Shaikjee, R. D. Hancock, *Inorg. Chem.* **1986**, *25*, 2992–3000; c) V. J. Thom, G. D. Hosken, R. D. Hancock, *Inorg. Chem.* **1985**, *24*, 3378–3381; d) V. J. Thöm, G. D. Hosken, R. D. Hancock, *J. Chem. Soc. Dalton Trans.* **1985**, 1877–1880; e) A. Andrés, A. Bencini, A. Charachalios, A. Bianchi, P. Dapporto, E. Garcia-España, P. Paoletti, P. Paoli, *J. Chem. Soc. Dalton Trans.* **1993**, 3507–3513.

[35] A. Bianchi, E. Garcia-España, *J. Chem. Educ.* **1999**, *76*, 1727–1732.

[36] C. Bazzicalupi, A. Beconcini, A. Bencini, V. Fusi, C. Giorgi, A. Masotti, B. Valtancoli, *J. Chem. Soc. Perkin Trans. 2* **1999**, 1675–1682.

[37] J. E. Richman, T. J. Atkins, *J. Am. Chem. Soc.* **1974**, *96*, 2268–2275.

[38] a) U. S. Schubert, C. Eschbaumer, M. Heller, *Org. Lett.* **2000**, *2*, 3373–3376; b) T. M. Cassol, F. W. J. Demnitz, M. Navarro, E. A. Neves, *Tetrahedron Lett.* **2000**, *41*, 8203–8206.

[39] A. Bencini, A. Bianchi, M. Micheloni, P. Paoletti, E. Garcia-España, *J. Chem. Soc. Dalton Trans.* **1993**, 1171–1174.

[40] P. Gans, A. Sabatini, V. Vacca, *Talanta* **1996**, *43*, 807–812.

[41] A. K. Covington, M. Paabo, R. A. Robinson, R. G. Bates, *Anal. Chem.* **1968**, *40*, 700–709.

[42] CrysAlis CCD, Oxford Diffraction Ltd., Version 1.171.32.5, **2008**.

[43] CrysAlis RED, Oxford Diffraction Ltd., Version 1.171.32.5, **2008**.

[44] M. C. Burla, R. Caliandro, M. Camalli, B. Carrozzini, G. L. Cascarano, L. De Caro, C. Giacovazzo, G. Polidori, R. Spagna, *J. Appl. Crystallogr.* **2005**, *38*, 381–388.

[45] G. M. Sheldrick, SHELXL-97, Göttingen, **1997**.

[46] a) M. W. Schmidt, K. K. Baldridge, J. A. Boatz, S. T. Elbert, M. S. Gordon, J. H. Jensen, S. Koseki, N. Matsunaga, K. A. Nguyen, S. Su, T. L. Windus, M. Dupuis, J. A. Montgomery, *J. Comput. Chem.* **1993**, *14*, 1347–1363; b) M. S. Gordon, M. W. Schmidt in *Theory and Applications of Computational Chemistry: The First Forty Years* (Eds.: C. E. Dykstra, G. Frenking, K. S. Kim, G. E. Scuseria), Elsevier, Amsterdam, **2005**, pp. 1167–1184.

[47] P. J. Hay, W. R. Wadt, *J. Chem. Phys.* **1985**, *82*, 270–283.

[48] W. J. Stevens, H. Basch, M. Krauss, *J. Chem. Phys.* **1984**, *81*, 6026–6033.

[49] a) A. D. Becke, *J. Chem. Phys.* **1993**, *98*, 5648; b) P. J. Stephens, F. J. Devlin, C. F. Chablowski, M. J. Frisch, *J. Phys. Chem.* **1994**, *98*, 11623–11627; c) R. H. Hertwig, W. Koch, *Chem. Phys. Lett.* **1997**, *268*, 345–351.

Received: February 2, 2009
Published online: June 5, 2009

